TKK Dissertations 89
Espoo 2007

HIGH-Q MECHANICAL SILICON OSCILLATORS IN OPTOMECHANICAL SENSOR APPLICATIONS

Doctoral Dissertation

Ossi Hahtela

Helsinki University of Technology
Department of Electrical and Communications Engineering
Micro and Nanosciences Laboratory

TKK Dissertations 89
Espoo 2007

HIGH-Q MECHANICAL SILICON OSCILLATORS IN OPTOMECHANICAL SENSOR APPLICATIONS

Doctoral Dissertation

Ossi Hahtela

Dissertation for the degree of Doctor of Science in Technology to be presented with due permission of the Department of Electrical and Communications Engineering for public examination and debate in Large Seminar Hall of Micronova at Helsinki University of Technology (Espoo, Finland) on the 26th of October, 2007, at 12 noon.

Helsinki University of Technology
Department of Electrical and Communications Engineering
Micro and Nanosciences Laboratory

Teknillinen korkeakoulu
Sähkö- ja tietoliikennetekniikan osasto
Mikro- ja nanotekniikan laboratorio

Distribution:
Helsinki University of Technology
Department of Electrical and Communications Engineering
Micro and Nanosciences Laboratory
P.O. Box 3500
FI - 02015 TKK
FINLAND
URL: http://www.micronova.fi/units/mns/
Tel. +358-9-4511
Fax +358-9-451 3128
E-mail: ossi.hahtela@tkk.fi

ISBN 978-951-22-8978-3
ISBN 978-951-22-8979-0 (PDF)
ISSN 1795-2239
ISSN 1795-4584 (PDF)
URL: http://lib.tkk.fi/Diss/2007/isbn9789512289790/

TKK-DISS-2349

Multiprint Oy
Espoo 2007

ABSTRACT OF DOCTORAL DISSERTATION	HELSINKI UNIVERSITY OF TECHNOLOGY P.O. BOX 1000, FI-02015 TKK http://www.tkk.fi
Author Ossi Hahtela	
Name of the dissertation High-Q mechanical silicon oscillators in optomechanical sensor applications	
Manuscript submitted 1st June 2007	Manuscript revised 17th September 2007
Date of the defence 26th October 2007	
☐ Monograph	☒ Article dissertation (summary + original articles)

Department	Electrical and Communications Engineering
Laboratory	Micro and Nanosciences Laboratory
Field of research	Microsystems
Opponent(s)	Prof. Helge E. Engan
Supervisor	Prof. Ilkka Tittonen
Instructor	

Abstract

Optical interferometry on a well-defined mirror surface is the most promising technique to reach a sufficient measurement sensitivity so that eventually the detection of various long-sought quantum mechanical phenomena of macroscopic objects would be possible. Such goals would be for example to observe gravitational waves, standard quantum limit (SQL) and true nonlocal entanglement of macroscopic objects. In this work, two very sensitive optomechanical sensors to detect extremely small displacements in the position of a moving cavity mirror were constructed and characterized. The first sensor configuration utilizes a microfabricated, high-reflectivity (HR)-coated torsional high-Q silicon oscillator as a moving rear mirror in a Fabry-Pérot interferometer. The position of the oscillator was measured using the Hänsch-Couillaud stabilization technique. This sensor setup was used to demonstrate experimentally that an additional intensity modulated laser beam can be used to optically actuate the mechanical resonance of a macroscopic silicon oscillator through radiation pressure and photothermal effects.

For the second optomechanical sensor, a novel high-Q mechanical silicon oscillator, which effectively vibrates in a non-tilting out-of-plane mode, was designed and fabricated. The benefit of this oscillator design, if compared to traditional flexural, torsional and many bulk acoustic mode oscillators, is that the action of weak forces is observed to cause only pure linear translation of the moving mirror without any tilting or deformation of the mirror surface. The resonance frequency and the Q value of the uncoated oscillator were f_0 = 27.5 kHz and Q = 100 000 (at p = 0.01 mbar and T = 300 K). This is the highest reported Q value for a non-tilting out-of-plane mode oscillator. The HR-coated non-tilting oscillator was then employed as a moving cavity mirror and the Pound-Drever-Hall method was used to stabilize the laser frequency to the high-finesse ($\mathcal{F}$ = 2 600) optical cavity and to measure oscillator mirror displacements at a femtometer level.

In addition, the effects of the atomic layer deposited (ALD) alumina thin films on the dynamic, thermomechanical and optical characteristics of a high-Q mechanical silicon oscillator were studied. It was demonstrated that ALD alumina films with thickness at least up to 100 nm can be deposited on microfabricated mechanical resonant structures without any degrading of the initially high mechanical quality of the resonance. This is of great importance when depositing functional, protective and optical thin films on sensitive micromechanical devices. It was also shown that thin ALD alumina films effectively stiffen the resonant structure leading to the increase in the resonance frequency with increasing the film thickness and that the temperature sensitivity of the resonance frequency decreases as the film thickness increases.

Keywords	high-Q oscillator, silicon, optomechanical coupling, optical actuation, atomic layer deposition		
ISBN (printed)	978-951-22-8978-3	ISSN (printed)	1795-2239
ISBN (pdf)	978-951-22-8979-0	ISSN (pdf)	1795-4584
Language	English	Number of pages	56+45
Publisher	Helsinki University of Technology, Micro and Nanosciences Laboratory		
Print distribution	Helsinki University of Technology, Micro and Nanosciences Laboratory		
☒ The dissertation can be read at http://lib.tkk.fi/Diss/2007/isbn9789512289790/			

VÄITÖSKIRJAN TIIVISTELMÄ	TEKNILLINEN KORKEAKOULU PL 1000, 02015 TKK http://www.tkk.fi
Tekijä Ossi Hahtela	
Väitöskirjan nimi Suurihyvyyslukuiset mekaaniset piivärähtelijät optomekaanisissa sensorisovelluksissa	
Käsikirjoituksen päivämäärä 1.6.2007	Korjatun käsikirjoituksen päivämäärä 17.9.2007
Väitöstilaisuuden ajankohta 26.10.2007	
☐ Monografia	☒ Yhdistelmäväitöskirja (yhteenveto + erillisartikkelit)
Osasto Sähkö- ja tietoliikennetekniikan osasto Laboratorio Mikro- ja nanotekniikan laboratorio Tutkimusala Mikrosysteemit Vastaväittäjä(t) Prof. Helge E. Engan Työn valvoja Prof. Ilkka Tittonen Työn ohjaaja	

Tiivistelmä

Optinen interferometria on lupaavin menetelmä saavuttaa riittävä mittausherkkyys, joka viimein mahdollistaisi makroskooppisten kappaleiden mittaamiseen liittyvien kvantti-ilmiöiden havainnoinnin. Tällaisia ilmiöitä ovat mm. gravitaatioaallot, mittauksen kvanttiraja (SQL) ja toisistaan erillään olevien kappaleiden kvanttimekaaninen kytkeytyminen (entanglement). Tässä työssä rakennettiin ja karakterisoitiin kaksi optomekaanista sensoria, jotka pystyvät mittaamaan erittäin pieniä kaviteettipeilin liikkeitä. Ensimmäisessä optomekaanisessa sensorissa käytettiin suurihyvyyslukuista torsionaalista mikromekaanista piivärähtelijää Fabry-Pérot interferometrin liikkuvana peilinä. Piivärähtelijän liikettä mitattiin Hänsch-Couillaud stabilointimenetelmän avulla. Tällä optomekaanisella sensorilla osoitettiin, että intensiteettimoduloitua lasersädettä voidaan käyttää makroskooppisen mekaanisen värähtelijän resonanssin optiseen herättämiseen säteilypaineen ja valotermisen vaikutuksen avulla.

Toista optomekaanista sensoria varten suunniteltiin ja valmistettiin täysin uudentyyppinen suurihyvyyslukuinen piivärähtelijä, joka värähtelee komponentin pinnantasoon nähden kohtisuorassa suunnassa. Tämän värähtelijärakenteen etu verrattuna perinteisiin taipuma-, kiertymä- ja tilavuusaaltovärähtelijöihin on se, että värähtelijään vaikuttava heikko mekaaninen voima aiheuttaa ainoastaan peilitason lineaarisen siirtymän ilman peilipinnan kiertymistä tai taipumista. Pinnoittamattoman piivärähtelijän resonanssitaajuus oli f_0 = 27.5 kHz ja hyvyysluku Q = 100 000 (p = 0.01 mbar ja T = 300 K). Kyseessä on korkein raportoitu Q-arvo tämän tyyppiselle värähtelijärakenteelle. Peilipinnoitettu piivärähtelijä asennettiin optisen kaviteetin liikkuvaksi peiliksi. Pound-Drever-Hall menetelmää käytettiin lukitsemaan laserin taajuus korkeafinessiseen ($\mathcal{F}$ = 2 600) optiseen kaviteettiin ja mittaamaan piivärähtelijän liikettä jopa femtometritasolla.

Lisäksi tutkittiin atomikerroskasvatettujen (ALD) alumiinioksidiohutkalvojen vaikutuksia suurihyvyyslukuisten mekaanisten piivärähtelijöiden dynaamisiin, lämpömekaanisiin ja optisiin ominaisuuksiin. Tässä työssä osoitettiin, että on mahdollista kasvattaa vähintään 100 nm paksuisia alumiinioksidiohutkalvoja mikromekaanisten värähtelijöiden pinnalle huonontamatta mekaanisen resonanssin hyvyyslukua. Tämä on hyvin tärkeä ominaisuus kasvatettaessa toiminnallisia, suojaavia ja optisia ohutkalvoja mikromekaanisten komponenttien pinnalle. Alumiinioksidikerrosten todettiin jäykistävän värähtelijärakennetta, minkä johdosta värähtelytaajuus kasvaa kalvon paksunemisen myötä. Värähtelytaajuuden riippuvuus lämpötilasta sen sijaan pieneni kun kalvoa kasvatettiin paksummaksi.

Asiasanat suurihyvyyslukuinen värähtelijä, pii, optomekaaninen kytkeytyminen, optinen heräte, atomikerroskasvatus	
ISBN (painettu) 978-951-22-8978-3	ISSN (painettu) 1795-2239
ISBN (pdf) 978-951-22-8979-0	ISSN (pdf) 1795-4584
Kieli englanti	Sivumäärä 56+45
Julkaisija Teknillinen korkeakoulu, Mikro- ja nanotekniikan laboratorio	
Painetun väitöskirjan jakelu Teknillinen korkeakoulu, Mikro- ja nanotekniikan laboratorio	
☒ Luettavissa verkossa osoitteessa http://lib.tkk.fi/Diss/2007/isbn9789512289790/	

PREFACE

The research work presented in this Thesis has been carried out at the Micro and Nanosciences Laboratory, Department of Electrical and Communications Engineering of Helsinki University of Technology during the years 2002-2007.

I would like to thank Professor Ilkka Tittonen for giving me the opportunity to work at the Microsystems group of the Micro and Nanosciences Laboratory. I am also very grateful for his supervision and guidance during the research work and writing process of this Thesis.

I am very grateful to my colleagues at Metrology Research Institute, Optics and Molecular Materials Laboratory and Micro and Nanosciences Laboratory for their contribution and assistance. Especially, I thank all the co-authors of the publications, Ms. Kaisa Nera and Ms. Päivi Sievilä for the fabrication of the silicon oscillators and Mr. Nikolai Chekurov for the FEM simulations. In addition, I thank Mr. Jyrki Pikkarainen from Optronics Department of Finnish Defence Forces and Mr. Aki Syväluoto from Oplatek Oy for the mirror coating of the silicon oscillators.

The National Graduate School of Electronics Production Technology and Reliability deserves acknowledgment for funding my graduate studies. Also the financial support by Ulla Tuominen Foundation is greatly acknowledged.

Most of all, I would like to express my sincere gratitude to my wife Leena for her love and patience and also my whole family and friends for their support and encouragement during the years.

Espoo, May 2007

Ossi Hahtela

TABLE OF CONTENTS

ABSTRACT 3

TIIVISTELMÄ 5

PREFACE 7

TABLE OF CONTENTS 8

LIST OF PUBLICATIONS 9

AUTHOR´S CONTRIBUTION 10

1 INTRODUCTION 11
1.1 Background 11
1.2 Aim and scope of the Thesis 13

2 MECHANICAL OSCILLATOR AS A MOVING MIRROR 15
2.1 Mechanical harmonic oscillator 15
2.2 Energy dissipation 17
2.3 Thermal noise 18
2.4 Fabrication 19
2.5 Torsional oscillator 20
2.6 Non-tilting out-of-plane mode oscillator 21
2.7 High-reflectivity coating 23
2.8 ALD alumina coating 24

3 OPTOMECHANICAL SENSING 29
3.1 Optomechanical coupling 29
3.2 Radiation pressure 29
3.3 Measurement of small displacements 31
3.4 Optical actuation 33

4 EXPERIMENTAL SETUPS 37
4.1 Hänsch-Couillaud stabilization 37
4.2 Pound-Drever-Hall stabilization 39
4.3 Michelson interferometry 43

5 DISCUSSION 45

6 SUMMARY 48

REFERENCES 50

LIST OF PUBLICATIONS

This Thesis consists of an overview and the following selection of the Author´s publications:

[I] O. Hahtela, K. Nera and I. Tittonen,
”Position measurement of a cavity mirror using polarization spectroscopy”,
J. Opt. A:Pure Appl. Opt. **6**, S115-S120 (2004).

[II] O. Hahtela and I. Tittonen,
”Optical actuation of a macroscopic mechanical oscillator”,
Appl. Phys. B **81**, 589-596 (2005).

[III] O. Hahtela, N. Chekurov and I. Tittonen,
”Non-tilting out-of-plane mode high-*Q* mechanical silicon oscillator”,
J. Micromech. Microeng. **15**, 1848-1853 (2005).

[IV] O. Hahtela and I. Tittonen,
”Non-tilting out-of-plane mode high-*Q* mechanical silicon oscillator as a moving cavity mirror”,
Appl. Phys. B **88**, 417-423 (2007).

[V] O. Hahtela, P. Sievilä, N. Chekurov and I. Tittonen,
”Atomic layer deposited alumina (Al_2O_3) thin films on a high-*Q* mechanical silicon oscillator”,
J. Micromech. Microeng. **17**, 737-742 (2007).

These publications are hereafter referred by their Roman numerals.

AUTHOR´S CONTRIBUTION

The research work presented in this Thesis has been carried out at the Micro and Nanosciences Laboratory of Helsinki University of Technology during the years 2002-2007. The Thesis consists of a short overview and five publications that are referred to as [I-V]. These publications are the results of group effort.

The manuscripts of all the Publications [I-V] have been written by the Author. The Author has designed and constructed the experimental setups presented in all the Publications [I-V]. The measurements and characterization of the silicon oscillators and optomechanical sensors have been performed by the Author. The Author is also responsible for the theoretical analysis and interpretation of the measurement results. The silicon oscillators used in Publications [I-V] have been fabricated by co-authors. In addition, the FEM simulation in Publication [III] and ALD alumina coating of the silicon oscillators in Publication [V] have been performed by the co-authors. The results reported in these publications have also been presented in several international conferences.

Other related publications to which the Author has contributed:

P. Sievilä, V.-P. Rytkönen, O. Hahtela, N. Chekurov, J. Kauppinen and I. Tittonen, ”Fabrication and characterization of an ultrasensitive acousto-optical cantilever”, *J. Micromech. Microeng*. **17**, 852-859 (2007).

1 INTRODUCTION

1.1 Background

Sensing, monitoring and controlling numerous physical properties of the environment are characteristic and essential in the modern information society. Different kinds of sensors are widely utilized in science and industry, for example in automobiles, machines, consumer electronics and medicine. Miniaturization of sensors increases integration and even portability. Technological progress in micro- and nanotechnologies over the past decades has enabled mass production of accurate, fast and reliable sensing devices. Novel sensing schemes appear every year at increasing speed.

Mechanical oscillators contain elements that typically vibrate in flexural (deflection), torsional or longitudinal (extensional, bulk) modes [1-3]. Small mechanical resonant structures are typically very sensitive to small changes in the physical parameters of the environment and especially to weak mechanical forces acting on them [4-7]. The response of a resonant system is proportional to the inverse of the resonance spectral width, which motivates the search towards systems that define the resonance very accurately. Narrow spectral width is characterized by a high Q value. In terms of dissipation, high Q means low energy losses, high resolution, accuracy and, because of the inherent weak coupling, long-term stability [8-11]. Therefore, high-Q micromechanical oscillators are commonly used as sensing elements in sensor applications and scientific instruments. High-Q oscillators can be used for example in realizing reference oscillators, filters, mixers, transmission lines and sensors for gas detection, acceleration, pressure and temperature. In addition, micro- and nanomechanical systems have been proposed to be used for the realization of ultra-sensitive detection devices [12] such as mass detection at a zeptogram-level [13,14] and force detection at an attonewton-level [15]. In most cases, the needed information of the measured quantity can be traced from the oscillator response as a change in the Q value, oscillation frequency, amplitude or phase.

Typically, a very sensitive and low-noise detection system is needed to accurately observe the response of a high-Q mechanical oscillator. In addition, the detection (and excitation) methods should not impair the performance or reliability of the device. Especially, it is important that the measurement technique does not degrade the initially high mechanical quality of the resonance for example by introducing extra damping or residual stresses. A convenient detection method is to use optical interferometry, in which a mechanical oscillator is integrated into an optical resonator as a moving mirror. In such a configuration, mechanical force typically introduces a change in the position of the oscillator mirror, which in turn induces a phase shift of the reflected optical field. Therefore, a phase-sensitive measurement of the reflected light provides information of the mirror displacement or, equivalently, information of the force acting on the mechanical oscillator. Such optical interferometric systems that utilize a moving cavity mirror are typically called optomechanical sensors (figure 1.1). Optomechanical effects

between coherent laser light and a moving cavity mirror can be utilized in a wide variety of high-precision sensing experiments such as in interferometric gravitational wave detection [16-18], atomic force microscopy (AFM) [19], optical cooling [20-23], optical actuation [24,25] and in various quantum optical schemes [26-33]. The use of highly reflecting cavity mirrors leads to a high optical finesse and enhancement of the optomechanical coupling so that extremely small displacements in the cavity mirror position can be detected. It should be noted that a Fabry-Pérot interferometer is sensitive to any length variations of the optical cavity whereas a high-Q mechanical oscillator is sensitive only to forces at its resonance frequency. Therefore, employing simultaneously a narrow mechanical resonance of a high-Q oscillator and a high-finesse optical cavity of a Fabry-Pérot interferometer, extremely good resonant force detection sensitivity can be achieved [34-36].

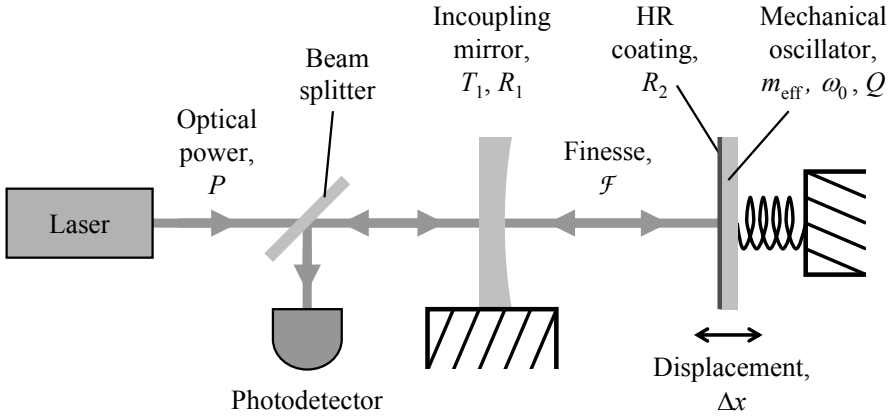

Figure 1.1 A simplified layout of an optomechanical sensor. Coherent laser light with optical power P enters an optical resonator (Fabry-Pérot interferometer) which consists of a stationary incoupling mirror and a moving rear mirror. Reflectivities of the mirrors determine the optical finesse $\mathcal{F}$ of the cavity. Typically, the moving mirror is modeled as a damped mechanical harmonic oscillator characterized by the effective mass m_{eff}, angular resonance frequency ω_0 and mechanical quality Q. The light reflected from the optical cavity is monitored with a photodetector.

At the quantum level, the measurement process always disturbs the system being measured [37]. The detection sensitivity in optical interferometric displacement measurements is ultimately limited by the quantum nature of light [16,37-39]. The fundamental sensitivity limit at which the position of an oscillator mirror can be measured is called standard quantum limit, SQL (see Chapter 3.3). A displacement measurement sensitivity of the order of the SQL is required for example in realizing gravitational wave detection experiments [16,17] and in schemes for demonstrating nonlocal entanglement of macroscopic objects [28,29]. A very good control of various noise sources is required when optomechanical systems are used to measure extremely small mirror displacements. In fact, reaching the SQL in an interferometric position measurement of a mechanical body has not yet been reported. Classical noise sources

such as thermal, acoustic, seismic and technical noise can easily mask the smallest mirror displacements. At room temperature experiments, the sensitivity of the optomechanical sensors is typically limited by thermal noise (Brownian motion) of the mirror. In order to reach a true quantum-limited behavior, a mechanical oscillator should be operated at very low temperatures, so that a condition $k_B T < \hbar\omega_0$ becomes valid. It is obvious that this is a very challenging requirement. For example if the resonance frequency is of the order of one megahertz, the oscillator should be cooled to the temperature of 50 μK. Besides cooling the mechanical oscillator to low temperatures, thermal noise effects can be reduced for example by using feedback control [20,40,41] or parametric amplification for squeezing of thermomechanical noise [42,43].

1.2 Aim and scope of the Thesis

The motivation for the research work summarized in this Thesis has been to investigate the potential of using optomechanically coupled high-*Q* mechanical silicon oscillators in high-precision sensing applications and design and fabricate new high-*Q* oscillators that are more suitable to be used in optical interferometric measurements. A closely related topic has been to study the effects of dielectric thin films on the performance and energy losses of high-*Q* mechanical oscillators.

Within this Thesis, two very sensitive optomechanical sensors, that are operated at low pressure and at room temperature, were constructed and characterized. The first sensor configuration utilizes a microfabricated, high-reflectivity (HR) -coated torsional high-*Q* mechanical silicon oscillator as a moving rear mirror in a Fabry-Pérot interferometer. The position of the oscillator mirror was measured using the Hänsch-Couillaud (HC) stabilization technique which is based on polarization spectroscopy [I]. This sensor setup was then used to demonstrate experimentally that an additional intensity modulated laser beam can be utilized to optically actuate the mechanical resonance of a macroscopic silicon oscillator through radiation pressure and photothermal effects [II]. For the second optomechanical sensor, a novel non-tilting out-of-plane mode high-*Q* mechanical silicon oscillator was designed and fabricated [III]. In this sensor configuration, the HR-coated non-tilting out-of-plane mode oscillator was employed as a moving cavity mirror and the Pound-Drever-Hall (PDH) method was used to stabilize the laser frequency to the high-finesse optical cavity and to measure oscillator mirror displacements [IV]. It is expected that this design will be used in various optical surface and near field studies.

Low energy losses and narrow spectral width of the mechanical oscillators are of great importance in high-precision sensing technology. One critical aspect is that, in many applications, one should be able to deposit protective, functional and optical thin films on sensitive micromechanical resonant structures without impairing the initially high mechanical quality of the resonance. Therefore, the effects of the atomic layer deposited (ALD) amorphous alumina (Al_2O_3) thin films on the dynamic, thermomechanical and optical characteristics of a high-*Q* mechanical silicon oscillator were studied [V].

The structure of the overview of this Thesis is as follows. Chapter 2 concentrates on discussing the relevant properties of high-Q mechanical silicon oscillators when they are used as moving mirrors in interferometric systems. The theory and limitations of the optomechanical coupling in the detection of weak forces and in displacement measurements are discussed in Chapter 3. This chapter also gives an introduction into optical actuation of mechanical oscillators using radiation pressure and photothermal effects. Chapter 4 describes the construction and operating principles of the experimental setups used in this work. Chapter 5 discusses the challenges related to the measurements of extremely small displacements of mechanical bodies and gives a short overview to the research activity in this field. Finally, Chapter 6 summarizes the results of this Thesis.

2 MECHANICAL OSCILLATOR AS A MOVING MIRROR

2.1 Mechanical harmonic oscillator

Mechanical silicon oscillators used in this Thesis can be modeled as a one-dimensional damped harmonic oscillator characterized by an effective mass m_{eff}, spring constant k and mechanical quality Q. Angular resonance frequency is determined by the spring constant and effective mass, $\omega_0 = 2\pi f_0 = (k / m_{\mathrm{eff}})^{1/2}$. The equation of motion under an external driving force at a frequency of ω is then given by

$$m_{\mathrm{eff}} \frac{\mathrm{d}^2 x(t)}{\mathrm{d}t^2} + \gamma \frac{\mathrm{d}x(t)}{\mathrm{d}t} + kx(t) = F_0 \cos(\omega t), \tag{2.1}$$

where $x(t)$ is the oscillator displacement as a function of time and γ is the damping constant. For a viscously-damped harmonic oscillation the damping constant is $\gamma = m_{\mathrm{eff}}\omega_0 / Q$. Although the energy dissipation of the high-Q oscillation mode is introduced mainly by the intrinsic losses rather than viscous (gas) damping in low pressure experiments, the use of viscous damping model is adequate because the oscillator response is mainly considered in the vicinity of the mechanical resonance frequency [44]. The solution of $x(t)$ can be written as [45]

$$x(t) = x_0 \mathrm{e}^{-\frac{\omega_0 t}{2Q}} \cos(\omega t + \phi) + |\chi(\omega)| F_0 \cos[\omega t + \delta(\omega)], \tag{2.2}$$

where the first term of the right-hand side is the transient part of the oscillator response corresponding to the exponentially damped harmonic oscillation (figure 2.1), x_0 is the oscillation amplitude and ϕ is a phase shift. The second term is the steady-state part of the solution, *i.e.* the frequency response of the oscillation (figure 2.2), and $\chi(\omega)$ is the mechanical susceptibility with a Lorentzian functional form,

$$\chi(\omega) = \frac{1}{m_{\mathrm{eff}}\left(\omega_0^2 - \omega^2 - \mathrm{i}\frac{\omega\omega_0}{Q}\right)}. \tag{2.3}$$

The frequency dependence of the phase $\delta(\omega)$ can be derived from

$$\tan[\delta(\omega)] = \frac{\omega\omega_0}{Q(\omega^2 - \omega_0^2)}. \tag{2.4}$$

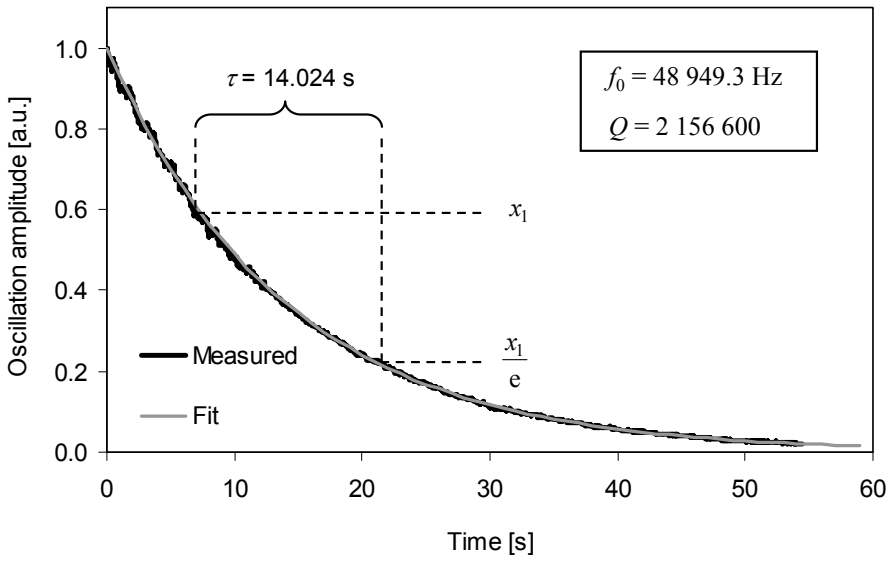

Figure 2.1 Measured and fitted decay curves of an uncoated torsional silicon oscillator. At a cryogenic temperature ($T = 4.2$ K), the decay time of the high-Q oscillation mode was $\tau = 14.024$ s yielding an extremely high mechanical Q value of $Q = 2\ 156\ 600$.

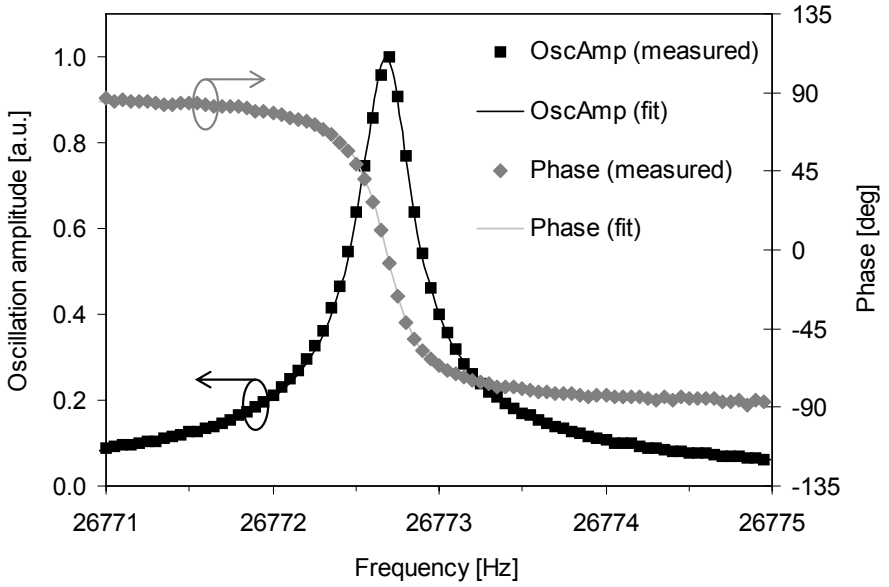

Figure 2.2 Measured frequency responses of the oscillation amplitude and phase of an uncoated non-tilting out-of-plane mode oscillator at $p = 0.1$ mbar and at room temperature. The solid lines refer to the fitted frequency responses according to equations (2.2) and (2.4).

2.2 Energy dissipation

High mechanical quality of the resonance, Q value, is a desired property in many high precision sensing applications. High Q value means spectrally narrow mechanical resonance and hence high-Q oscillators typically provide very good frequency resolution and stability. A mechanical oscillator can be considered as a bandpass filter which rejects excitation at frequencies outside its bandwidth [46]. Thus, a high Q value leads to an excellent decoupling from other undesired vibrational modes and external noise sources. In addition, high Q value indicates low energy losses and, therefore, high-Q oscillators can be used to realize devices with potentially very low power consumption. In order to reach a high Q value, one should try to minimize the energy dissipation by selecting a suitable oscillator structure, oscillation mode and material.

The Q value is determined as a ratio between the total energy E_0 stored in the oscillation and energy dissipation ΔE per oscillation cycle. In frequency domain, this is equivalent to the ratio between resonance frequency f_0 and spectral width of the resonance Δf. In time domain, Q value can be determined from the resonance frequency and decay time τ corresponding to the oscillation amplitude being decreased to (1/e)th part of its initial value. Thus, Q value can be written as

$$Q = \frac{2\pi E_0}{\Delta E} = \frac{f_0}{\Delta f} = \pi \tau f_0 \,. \tag{2.5}$$

The total energy dissipation per oscillation cycle is a sum of various internal and external loss mechanisms and the total Q value can be derived from

$$\frac{1}{Q} = \frac{1}{Q_\mathrm{i}} + \frac{1}{Q_\mathrm{s}} + \frac{1}{Q_\mathrm{v}} \,, \tag{2.6}$$

where Q_i is determined by the internal losses, Q_s is related to energy losses through the oscillator support structure (clamping losses) and Q_v is due to the viscous and acoustic losses to the surrounding medium (gas damping).

Internal losses are related to physical deformations of the oscillator structure. A bulk silicon crystal may dissipate mechanical energy for example due to internal friction, phonon-phonon interactions and by phonon scattering from impurities and dislocations [47]. Another internal loss mechanism is the thermoelastic dissipation in which local changes in the volume due to the oscillator deformation lead to irreversibly transformed thermal energy [8,48]. It has been demonstrated that the Q value is strongly dependent on the surface effects of the oscillator and energy losses seem to increase proportional to increasing the surface-to-volume ratio [9,49].

Gas damping of the surrounding medium is the main source of external energy losses of high-Q mechanical oscillation. Close to atmospheric pressures the surrounding gas acts as if it were a viscous fluid and some of the oscillation energy is lost through friction

and acoustic coupling. The energy dissipation due to the surrounding gas becomes naturally less significant at low pressure and is negligible below $p = 10^{-3}$ mbar (figure 2.3) [9]. At resonance, a mechanical oscillator vibrates in a standing wave pattern. Some of the vibrational energy is inevitably lost through the support structures. In order to minimize such clamping losses, the motion of the support structures should be minimized [50]. Therefore, one should place the supports at nodal points of the oscillation mode.

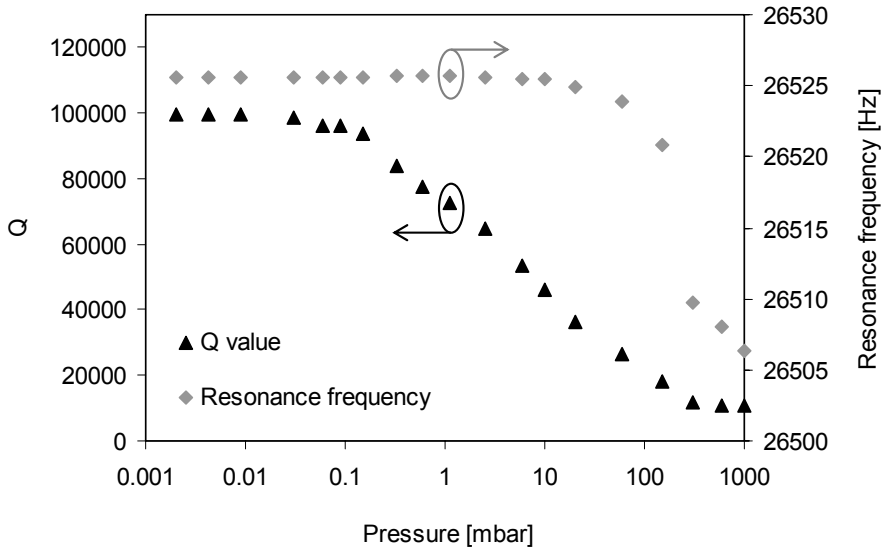

Figure 2.3 Measured Q value and resonance frequency of an uncoated non-tilting out-of-plane mode oscillator as a function of pressure at room temperature.

2.3 Thermal noise

Thermal noise can be the dominating noise component in many experiments that use a mechanical oscillator and that require high precision and sensitivity [44,51]. The fluctuation-dissipation theorem states that the dissipation in silicon oscillator couples the thermal energy of the environment (thermal bath) to the mechanical motion (fluctuation) of the oscillator. In other words, thermal energy produces a random excitation force to the oscillator, which causes fluctuations in the oscillator position known as Brownian motion (figure 2.4).

When a classical one-dimensional harmonic oscillator is in thermal equilibrium with its environment at temperature T, it possesses an average energy of $k_B T / 2$. According to the equipartition theorem [44], this thermal energy is related to the thermally excited noise in the oscillator position (Brownian motion) as

$$\frac{1}{2} m_{\text{eff}} \omega_0^2 \Delta x_{\text{th}}^2 = \frac{1}{2} k_B T , \tag{2.7}$$

where Δx_{th} is thermally induced rms oscillation amplitude. The spectral density of the thermal fluctuation in the oscillator position $S_{th}(\omega)$ in units of m^2 / Hz is given by

$$S_{th}(\omega) = |\chi(\omega)|^2 S_F(\omega) = |\chi(\omega)|^2 \frac{4k_B T m_{eff} \omega_0}{Q}, \tag{2.8}$$

where $S_F(\omega)$ is the Langevin force responsible for the thermomechancial excitation.

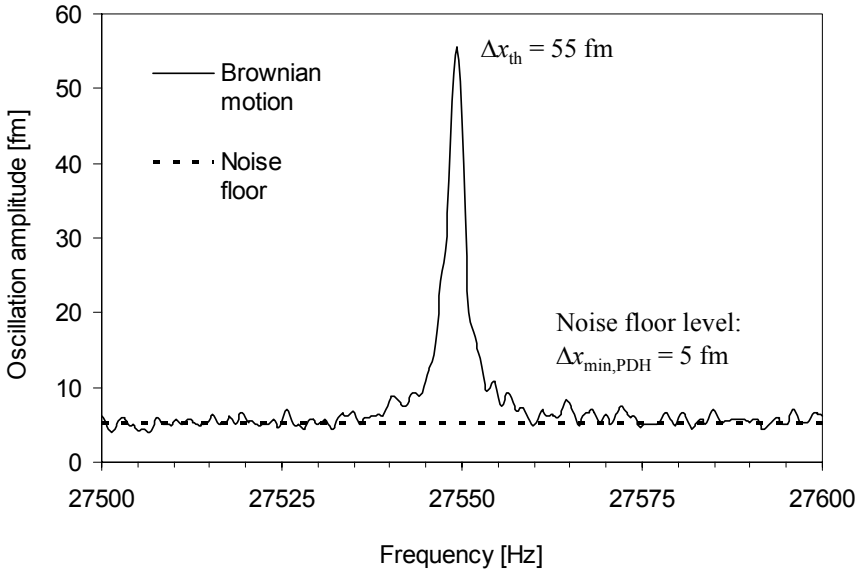

Figure 2.4 Frequency response of a HR-coated non-tilting out-of-plane mode oscillator in thermal equilibrium at T = 300 K. In this case, thermally induced Brownian motion at resonance was Δx_{th} = 55 fm. The noise floor next to the resonance peak determines the displacement measurement sensitivity of the PDH-stabilized optomechanical sensor, $\Delta x_{min,PDH}$ = 5 fm (see Chapter 4.2).

2.4 Fabrication

The oscillator material has a significant influence on the internal energy loss mechanisms of the oscillator. In this Thesis, single-crystal silicon was chosen because it has low intrinsic losses and excellent elastic properties [52]. Since 1950s, silicon has been the most common material in semiconductor industry and its mechanical, electrical and optical properties are well known. High-quality single-crystal silicon wafers are easily available. High purity of the material and highly regular lattice structure lead to reliable and stable mechanical structures. Established microfabrication processes are sufficient for the fabrication of high-Q oscillators [53]. Single-crystal silicon is anisotropic material meaning that various material properties depend on the particular crystallographic direction. This property also allows the use of anisotropic etchants for shaping three-dimensional structures [10,53].

In this work, the oscillators were fabricated in the clean room facilities of *Micronova* at *Helsinki University of Technology*. Double-sided polished (DSP) 380-μm thick (100) oriented single-crystal silicon wafers (p-type, 5-10 Ω cm) were used. A thermally grown silicon dioxide (SiO_2) layer was utilized as an etch mask. The oscillators were patterned by double-sided UV-lithography and the structures were released by using double-sided anisotropic wet etching in a 25 % tetra-methyl ammonium hydroxide (TMAH) solution at 85 °C. Such a fabrication process has the benefit of allowing well-defined symmetric features and high surface quality which are required for reaching a balanced oscillation mode and low damping of mechanical energy.

A three-dimensional finite-element model (FEM) of the oscillators was utilized to identify the vibrational mode patterns and resonance frequencies of the high-Q mode oscillations. Although the exact numerical Q value cannot be predicted by the FEM simulation, it is still a useful method to estimate the damping of mechanical energy in different vibrational modes because it reveals the strain concentration and stress maxima points generated in the oscillator structure. Therefore, FEM simulations can be used to give guidance in optimizing oscillator design for obtaining low damping and high Q values [11,54].

2.5 Torsional oscillator

Torsional oscillators with a high Q value have proven to be very feasible and powerful instruments in a wide variety of measurement applications [4,11,34,45,52,55-60]. A balanced torsional mode oscillation typically introduces very little internal damping leading to a high Q value. There is no considerable local volume changes present in a weak torsional motion meaning that thermoelastic losses are negligible [2,9]. In addition, the coupling to the clamping losses and external vibrations is rather low because the center of mass of the oscillator stays stationary during the torsional oscillation [4,9].

The torsional silicon oscillator design used in Publications [I] and [II] is illustrated in figure 2.5. In this design the actual oscillator is a balanced torsionally vibrating rectangular silicon vane ($1.4 \times 2.3 \times 0.38$ mm^3) which is mounted with narrow bridges to several surrounding frames. The purpose of combining several frames around the oscillator is to minimize the clamping losses by decoupling the oscillating vane from the support structure [2]. In principle, the additional frames are torsionally vibrating oscillators as well but due to the much larger mass their resonance frequencies differ considerably from that of the inner vane resonance and are thus sufficiently decoupled from the high-Q mode oscillation. The resonance frequency and Q value of the uncoated torsional silicon oscillators are about $f_0 = 67.7$ Hz and $Q = 750\,000$ at low pressure ($p = 10^{-3}$ mbar) and at room temperature. At a cryogenic temperature of $T = 4.2$ K, the highest measured Q value for a similar torsionally vibrating structure was $Q = 2\,156\,000$ (figure 2.1).

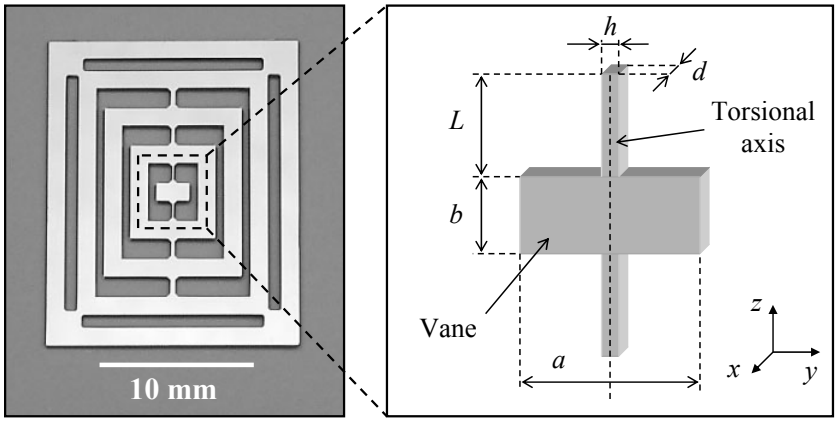

Figure 2.5 Torsional mechanical silicon oscillator. The parameters determining this design are a = 2.3 mm, b = 1.4 mm, h = 200 μm, d = 380 μm and L = 1.2 mm.

In torsional oscillation, the oscillator is rotated around its torsional axis (figure 2.5). The equation of angular motion for a torsional mechanical oscillation is

$$\Theta \frac{\mathrm{d}^2\theta(t)}{\mathrm{d}t^2} + \gamma_\mathrm{t} \frac{\mathrm{d}\theta(t)}{\mathrm{d}t} + \kappa\theta(t) = \tau(t), \tag{2.9}$$

where Θ is the mass moment of inertia of the torsional oscillation, $\theta(t)$ is the rotation angle, γ_t is the torsional damping constant, κ describes the torsional restoring constant of the two silicon bridges and $\tau(t)$ is external torque. The oscillator size parameters and the density of silicon ρ_Si determine the mass moment of inertia

$$\Theta = \frac{2}{3}\rho_\mathrm{Si}\left(\frac{a}{2}\right)^3 bd\,, \tag{2.10}$$

where parameters a, b and d are as described in figure 2.5. In addition, the mass moment of inertia can be used to determine the effective mass of the torsional oscillator $m_\mathrm{eff} = \Theta / l^2$ at the distance l off the torsional axis.

2.6 Non-tilting out-of-plane mode oscillator

Torsional motion possesses the inherent tilting of the oscillator vane which may cause some problems in certain applications. In some experiments, it is desirable that the motion of a mechanical oscillator takes place precisely in a direction that is normal to the oscillator surface. If a torsional oscillator is employed as a mirror in an interferometric system, torsional motion inevitably introduces deflection of the reflected light. This may impair or forbid the optical cavity mode stabilization, especially when large oscillation amplitudes or long optical cavities are used. In principle, the excitation

of a torsional oscillation requires a torsional force, *i.e.* torque, on the oscillator. This may set limitations to the type of force that can be detected with a torsional oscillator. For example, if the studied force can be considered as a plane wave with a large cross-section compared to the oscillator surface area, the torsional oscillation mode may not become effectively excited. When studying short-range interactions of surfaces, such as Casimir force of two conducting plates [61-65] with a micromechanical oscillator, the oscillating element should be kept parallel to the other surface. In addition, such experiments typically require very small separation between the surfaces which limits the use of torsional motion. In order to overcome certain drawbacks related to oscillators vibrating in a torsional mode, a mechanical oscillator which effectively vibrates in a non-tilting out-of-plane mode but still has a substantially high Q value was designed and fabricated [III].

The non-tilting out-of-plane mode oscillator is illustrated in figure 2.6(a). The oscillator body ($1.5 \times 14 \times 0.38$ mm^3) is basically a free-free beam vibrating in a second flexural mode. Figure 2.6(b) shows the result of the FEM simulation of the non-tilting out-of-plane oscillation mode. The oscillator body is mounted from its central nodal point to the frame with two torsional suspension bars. Ideally, the suspension bars experience only torsional motion in the high-Q mode oscillation. The effective lengths of the suspension bars correspond to the quarter wavelength of the resonance frequency of the high-Q mode oscillation. Thus, the suspension bars act as impedance matched acoustic transmission lines and the oscillation experiences minimum energy dissipation through the supports [1]. The advantage of inserting additional masses on the thin torsional suspension bars is that one can use shorter suspension bars and gain a mechanically robust structure. The two rectangular vanes ($0.8 \times 0.8 \times 0.38$ mm^3) are mounted with narrow bridges to the oscillator body. The mounting of the vanes is accurately positioned to the antinodes of the body. Thus, the vanes vibrate in anti-phase relative to each other and exactly parallel to their rest position during the whole vibration cycle. At low pressure ($p = 10^{-3}$ mbar) and at room temperature, the resonance frequency and Q value of the uncoated non-tilting out-of-plane mode oscillators are about $f_0 = 27$ kHz and $Q = 100\,000$, respectively. This is the highest reported Q value for a non-tilting out-of-plane mode oscillator.

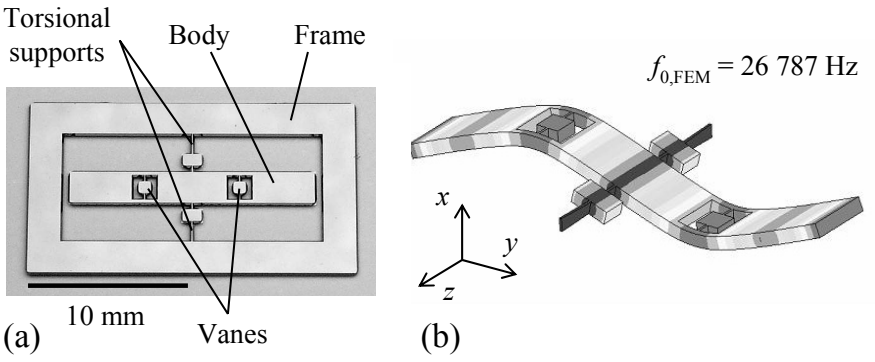

Figure 2.6 (a) Photograph of the non-tilting out-of-plane mode high-Q mechanical silicon oscillator. (b) Vibrational mode pattern of the high-Q mode oscillation given by the FEM simulation.

If the surrounding openings of the vanes are excluded, the oscillator body can be considered as a uniform free-free beam which vibrates in the second flexural mode. The characteristic function $x_n(y)$ gives the mode pattern, *i.e.* the oscillation amplitudes along the y-axis, of the nth oscillation mode [66]

$$\begin{aligned} x_n(y) = A_n[&(\cos\beta_n L - \cosh\beta_n L)(\sin\beta_n y + \sinh\beta_n y) \\ &-(\sin\beta_n L - \sinh\beta_n L)(\cos\beta_n y + \cosh\beta_n y)] \end{aligned}, \tag{2.11}$$

where A_n is a constant, L is the length of the free-free beam and $\beta_n L$ is a parameter related to the nth flexural mode of the free-free beam obtained by numerically solving the equation

$$\cos\beta L \cosh\beta L = 1. \tag{2.12}$$

For the second flexural mode $\beta_2 L = 7.8532$. Because the length L of the oscillator body is much larger than the width w and thickness h (*i.e.* $L >> w$ and $L >> h$), the resonance frequency of the nth flexural mode can be determined according to the Euler-Bernouli beam theorem [66] by

$$f_0 = \frac{(\beta_n L)^2}{2\pi}\frac{h}{L^2}\sqrt{\frac{E_{\mathrm{Si}}}{12\rho_{\mathrm{Si}}}}, \tag{2.13}$$

where E_{Si} and ρ_{Si} are the Young´s modulus and density of silicon, respectively.

2.7 High-reflectivity coating

Both torsional and non-tilting out-of-plane mode oscillators were used as a planar rear mirror in Fabry-Pérot interferometers. In order to achieve a high optical finesse, a high-reflectivity (HR) coating was deposited on the silicon oscillators by sputtering numerous sequential dielectric quarter-wave layers of titanium dioxide (TiO_2) and silicon dioxide (SiO_2). The HR coating of the torsional oscillator was optimized for the HeNe laser wavelength of $\lambda = 633$ nm [67]. The reflectivity of the HR coating was $R = 0.98$ and the total thickness of the HR coating was 1.14 µm. The deposition of the relatively thick HR coating resulted in a significant increase in mechanical losses and consequently the Q value was reduced from $Q = 750\,000$ for an uncoated torsional oscillator to $Q = 42\,000$ after HR coating. Both values were measured at low pressure ($p = 10^{-2}$ mbar) and at room temperature. The resonance frequency of the torsional oscillator was decreased an amount of 70 Hz (*i.e.* 0.1 %) due to the increased mass and change in the effective stiffness of the coated oscillator.

In the case of non-tilting out-of-plane mode oscillators, the HR coating was optimized for the Nd:YAG laser ($\lambda = 1064$ nm) and the achieved reflectivity was substantially higher, $R = 0.9977$ [68]. The total thickness of the HR coating was over 4 µm. In

addition, the back-side of the oscillator was coated with an anti-reflectivity (AR) coating to prevent unwanted reflections at the silicon-air interface behind the optical cavity. As a result of the coating, the Q value was decreased from $Q = 100\,000$ to $Q = 26\,000$ measured again at low pressure ($p = 10^{-2}$ mbar) and at room temperature. The resonance frequency was decreased by 40 Hz (*i.e.* 0.15 %) due to the relatively thick HR and AR coatings.

2.8 ALD alumina coating

Thin film-coated MEMS components are increasingly utilized in a vast variety of mechanical, electrical and optical device applications [69-72]. Many MEMS gas and mass sensors are based on functional thin film coatings that are deposited on the device. On the other hand, protective thin film coatings can be utilized to minimize or prevent certain problems such as mechanical wear, oxidation and short-circuiting [73]. In optical applications, thin film coatings and multilayer stacks may serve as either AR or HR coatings, filters and polarizers. In many cases, it is of great importance that such thin film coatings do not have a significant effect on the initially high mechanical quality of the MEMS devices. Therefore, the influence of the atomic layer deposited (ALD) alumina (Al_2O_3) thin films on the dynamic, thermomechanical and optical characteristics of the silicon oscillators were studied [V].

ALD growth is based on sequential self-limiting surface reactions [74,75]. Thus, the deposited film thickness can be controlled at the atomic level. Growing of the film is extremely linear and directly proportional to the number of individual deposition cycles [76,77]. ALD is an especially convenient technique to deposit uniform and conformal thin films on MEMS devices because they typically involve complex topography with small gaps, high aspect ratio trenches and shaded areas. Also the surface quality of ALD films is extremely good. Alumina has many favorable properties as thin film coating material. Alumina is hard and stiff with a high Young´s modulus [78]. It has good thermal and chemical stability, firm adhesion to many surfaces [73,79], high dielectric constant and excellent insulating properties [73,80]. In addition, it is optically transparent in a wide range of wavelengths [81] and it can be used as a low refractive index material [76] in dielectric coatings.

In this work, the alumina thin films were deposited on silicon oscillators using trimethyl aluminum ($Al(CH_3)_3$, TMA) and water as precursors. The deposition temperature and pressure in the ALD reactor were $T_{ALD} = 220$ °C and $p_{ALD} = 2.3$ mbar, respectively. Deposited film thicknesses varied from 5 nm to 662 nm. It was found that ALD alumina films effectively stiffen the resonant structure leading to the increase in the resonance frequency with increasing the film thickness (figure 2.7). If the non-tilting out-of-plane mode silicon oscillator is modeled as a uniform beam with rectangular cross-sections and it is coated on all sides with a thin uniform alumina film of thickness t, the resonance frequency can be approximated by using equation [82]

$$f_c = \frac{(\beta_n L)^2}{2\pi}\frac{h}{L^2}\sqrt{\frac{E_{Si}\frac{wh}{12} + E_A\left(\frac{w}{2}+\frac{h}{6}\right)t}{\rho_{Si}wh + 2\rho_A(w+h)t}}, \tag{2.14}$$

where L, w and h are the length, width and thickness of the uncoated oscillator body, respectively. E_{Si} and ρ_{Si} are Young´s modulus and density of the silicon and E_A and ρ_A are Young´s modulus and density of the ALD alumina, respectively. The increase in the resonance frequency is very linear when the film thickness is small compared to the thickness of the silicon oscillator. Young´s modulus of the ALD alumina was determined to be E_A = 177 GPa by fitting equation (2.14) on the experimental data of f_c with variable film thickness.

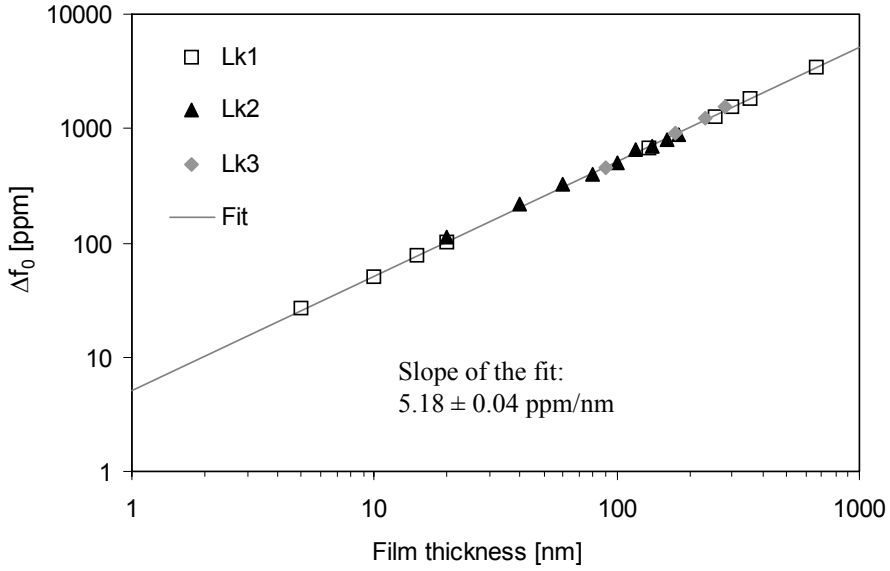

Figure 2.7 Deviation in the mechanical resonance frequency of the oscillators as a function of alumina film thickness. Three silicon oscillators (Lk1, Lk2 and Lk3) with various alumina film thicknesses were used. The solid line shows a fitting according to equation (2.14), yielding Young´s modulus of ALD alumina of E_A = 177 GPa.

The Q value of the non-tilting out-of-plane mode oscillation was determined as a function of the alumina film thickness (figure 2.8). It was shown that alumina films with thicknesses up to 100 nm had no significant influence on the Q value of the mechanical resonance. This was rather unexpected because earlier measurements have shown that mechanical quality of balanced and low loss high-Q structures is very sensitive to additional deposited films on the device [2,83]. The results presented in Publication [V] imply that ALD alumina itself has low internal friction and it is a potential choice of material for high-Q devices. If compared to other chemical vapor deposition (CVD) techniques, the ALD allows for the film growth at relatively low temperatures (35-500 °C) [70,76]. In addition, the oscillators are uniformly coated on all sides and the

difference in thermal expansion coefficients of silicon and ALD alumina is small (α_{Si} = 3 ppm K^{-1} [84], α_A = 5 ppm K^{-1} [85]). Therefore, thermomechanical-based stress is expected to be low at the film-substrate boundary. The additional alumina films change the resonance frequency of the oscillator body and, in this case, it seems that the impedance mismatch of the torsional support structure starts to impair the *Q* value when the alumina film thickness exceeds about 100 nm [V].

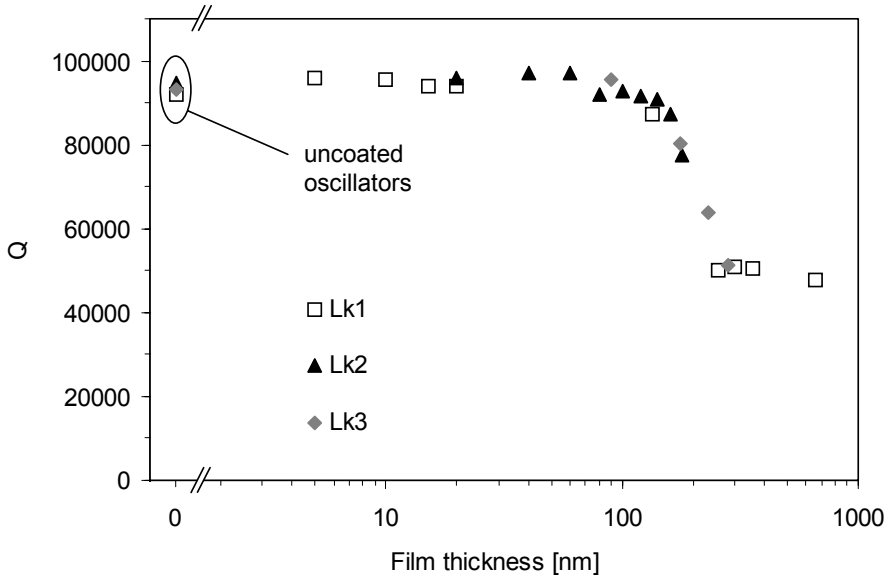

Figure 2.8 *Q* value measured as a function of the alumina film thickness at low pressure ($p = 10^{-2}$ mbar) and at room temperature. Three silicon oscillators (Lk1, Lk2 and Lk3) with various alumina film thicknesses were used.

Silicon has a negative temperature coefficient for the Young´s modulus. Therefore, the resonance frequency of silicon oscillators decreases at higher temperatures. However, in our measurements, the use of ALD alumina coating on a silicon oscillator results in a decrease in the temperature sensitivity of the resonance frequency with increasing film thickness. For the silicon oscillator with a 662-nm thick ALD alumina coating, the temperature-induced drift in the resonance frequency was 31% less than that of an uncoated silicon oscillator (figure 2.9). Therefore, ALD alumina coated silicon components can be utilized for example in realizing temperature insensitive sensors, reference oscillators and filters.

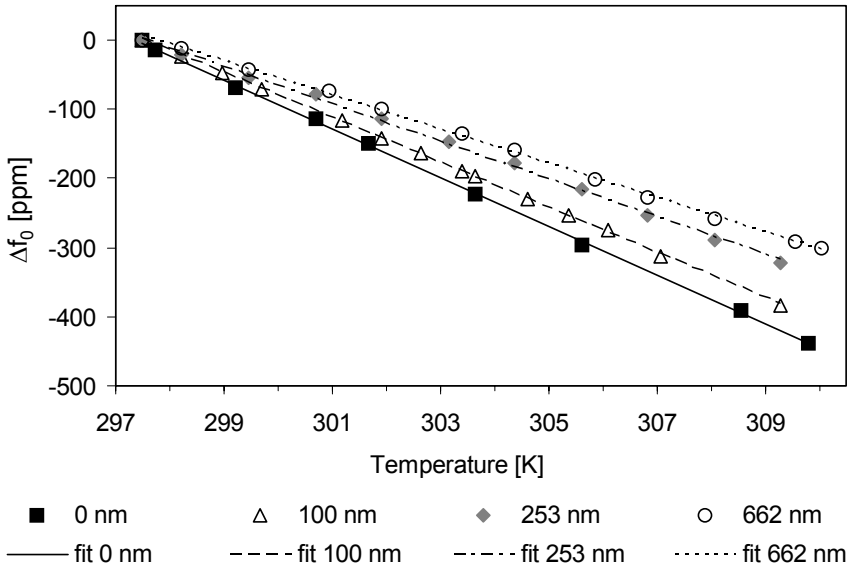

Figure 2.9 Deviation in the resonance frequency as a function of the ambient temperature for an uncoated silicon oscillator and for alumina-coated oscillators with film thicknesses of 100 nm, 253 nm and 662 nm. The added lines show linear fittings to the measurements.

ALD alumina can be used as a low refractive index material in optical coatings and multilayer stacks. The refractive index of ALD alumina thin films depends slightly on the growth process parameters and in our case $n_A = 1.64$ at the HeNe laser wavelength of $\lambda = 633$ nm. If a substrate is coated with a thin film, the incident light undergoes multiple reflections at both interfaces. The relative phase shift between these reflections depends on the thickness t and refractive index n_2 of the thin film. The total reflectivity at normal incidence is given by

$$R_{\mathrm{tot}} = \frac{R_{12} + R_{23} + 2\sqrt{R_{12}R_{23}}\cos\left(\frac{4\pi t n_2}{\lambda}\right)}{1 + R_{12}R_{23} + 2\sqrt{R_{12}R_{23}}\cos\left(\frac{4\pi t n_2}{\lambda}\right)}, \tag{2.15}$$

where R_{12} is the reflectivity at the boundary of the initial medium and the thin film and R_{23} is the reflectivity at the boundary of the thin film and the substrate. Figure 2.10 shows the reflectivity of the alumina-coated silicon oscillator as a function of the alumina film thickness. The measured values of reflectivity correspond very well to the theoretical calculations based on equation (2.15). A thin film serves as a single-layer AR coating if its refractive index is lower than that of the substrate. It was shown that ALD alumina thin films on silicon substrates can be used as a single-layer AR coating, offering a significant reduction in the reflectivity from $R_{\mathrm{Si}} = 0.35$ for a clean silicon

surface to $R_{AR} = 0.035$ for a silicon surface with a quarter wavelength alumina coating at $\lambda = 633$ nm.

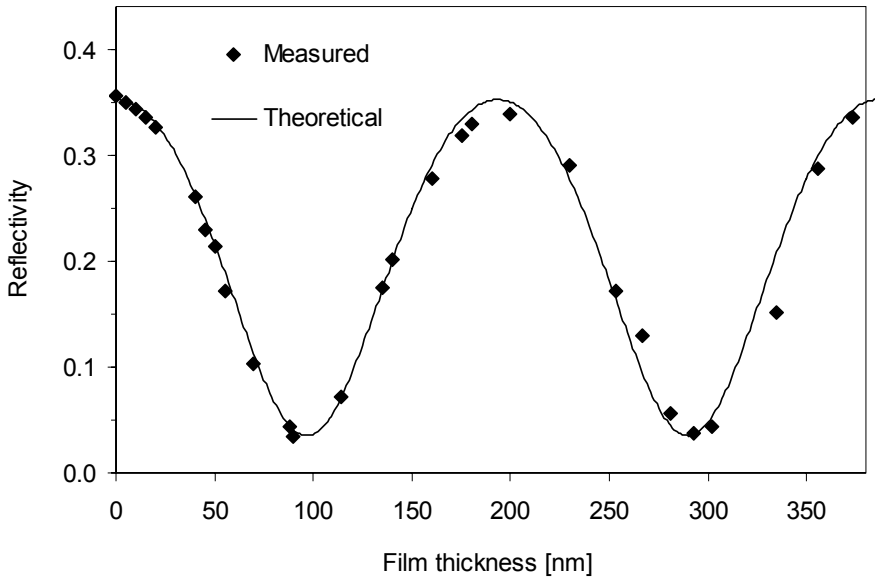

Figure 2.10 Reflectivity of the alumina-coated silicon oscillator at $\lambda = 633$ nm as a function of the film thickness. The refractive index of the ALD alumina film was $n = 1.64$. Measured data corresponds very well to the theoretical reflectivity calculated from equation (2.15).

3 OPTOMECHANICAL SENSING

3.1 Optomechanical coupling

Optomechanical effects can be utilized in a wide variety of high-precision sensing experiments such as in interferometric gravitational wave detection [86], atomic force microscopy (AFM) [87], optical cooling [20-23,88], optical actuation [58] and in various quantum optical schemes [26-32]. The radiation pressure acting on a moving mirror introduces an optomechanical coupling between the optical modes of the incident light and the mechanical vibrational modes of the mirror [30,31,43]. Optomechanical coupling experiments are typically realized by using a Fabry-Pérot interferometer with a stationary incoupling mirror and a moving end mirror. Extremely sensitive interferometric measurements related to inherently very weak optomechanical effects require also the active stabilization of the laser frequency to the optical cavity. Such a measurement configuration is referred to as an optomechanical sensor. A high finesse of the optical cavity can be used to enhance the optomechanical coupling so that extremely small displacements of the cavity mirror can be detected [34-36]. In many experiments, the moving end mirror is a HR-coated mechanical oscillator with a high Q value. It has been proposed that employing a high-Q mechanical oscillator as a moving mirror in a high-finesse optical cavity could even allow the demonstration of true nonlocal quantum effects with macroscopic systems [26] and implementation of quantum-limited displacement measurements of a mechanical body [34,37].

When coherent monochromatic light is incident on a Fabry-Pérot interferometer, the light will experience a maximum transmission through the optical cavity only if the cavity length L corresponds to the integer multiple of half wavelength of light. Thus, the difference between two sequential transmission peaks, the free spectral range (FSR), corresponds to the half wavelength variation in the cavity length. In frequency domain, free spectral range is given by $\Delta f_{\mathrm{FSR}} = c / 2L$. Consequently, an interferometric displacement measurement can be calibrated by using the FSR as a length reference. The finesse $\mathcal{F}$ is determined as a ratio of the free spectral range to the spectral width of the transmission peak, $\mathcal{F} = \Delta f_{\mathrm{FSR}} / \Delta f_{\mathrm{h}}$. Equally, the finesse can also be derived from the power reflectivity R of the cavity mirrors, $\mathcal{F} = \pi R^{1/2} / (1-R)$. Generally speaking, the sensitivity of the optomechanical sensor to detect small displacements in the position of the mirror increases with the finesse.

3.2 Radiation pressure

As the laser beam is incident on the oscillator surface, the oscillator is exposed to the mechanical momentum transferred by the reflected and absorbed photons [89]. The photons that reflect from the oscillator surface transfer a mechanical momentum p_{rad},

$$p_{\mathrm{rad}} = 2\hbar k\cos\theta = 2\frac{h}{\lambda}\cos\theta\,, \tag{3.1}$$

where $\hbar$ is Planck´s constant, k is the wave number, λ is the wavelength and θ is the angle of the incident beam with respect to the normal direction. Absorbed photons transfer mechanical momentum that is half of the momentum transferred by the reflected photons. The mean number of photons n incident on the oscillator surface per unit time can be derived from the optical power, $P = nhf = nhc / \lambda$, where hf is the energy per photon. The radiation pressure force applied to the oscillator due to the transferred mechanical momentum is [25]

$$F_{\mathrm{rad}} = \left[2R + (1-R)\right]n\frac{h}{\lambda}\cos\theta = (1+R)\frac{P}{c}\cos\theta\,, \tag{3.2}$$

where R is the power reflectivity of the oscillator mirror and $1 - R$ is the absorbed fraction of the incident light. An intensity-modulated laser beam can be utilized to optically actuate the resonance of a mechanical oscillator. The displacement of the oscillator $\Delta x_{\mathrm{rad}}(\omega)$ due to a modulated monochromatic radiation pressure force $F_{\mathrm{rad}}(\omega)$ is

$$\Delta x_{\mathrm{rad}}(\omega) = |\chi(\omega)|F_{\mathrm{rad}}(\omega) = |\chi(\omega)|(1+R)\frac{P(\omega)}{\mathrm{c}}\cos\theta\,. \tag{3.3}$$

The impact of each incident photon hitting the oscillator surface can be seen as a propulsive force trying to push the oscillator away from the light source. Therefore, in order to actuate harmonic motion, a dc optical power component P_{dc} must be involved. The dc optical power causes a small static deflection in the oscillator position, which can be considered as a new equilibrium position around which the oscillator is vibrating when the intensity-modulated laser beam is applied. The displacement due to the constant radiation pressure $F_{\mathrm{rad,dc}}$ is

$$\Delta x_{\mathrm{rad,dc}} = \frac{F_{\mathrm{rad,dc}}}{k} = (1+R)\frac{P_{\mathrm{dc}}}{m_{\mathrm{eff}}\omega_0^2 c}\cos\theta\,. \tag{3.4}$$

In addition, the shot noise of laser light introduces an uncertainty in the oscillator position through an additional radiation pressure noise. Shot noise is based on the quantum nature of light and it arises from the fluctuations in the number of photons n. Because of the Poisson distribution, the standard deviation of the number of photons is equal to the square root of the mean number of photons in a laser beam, $\sigma_{\mathrm{n}} = n^{1/2}$. The square root of the spectral power density S_{SN} of the shot noise is

$$\sqrt{S_{\mathrm{SN}}} = \sigma_{\mathrm{n}} hf = \sqrt{\frac{P\lambda}{hc}}\frac{hc}{\lambda} = \sqrt{\frac{Phc}{\lambda}}\,. \tag{3.5}$$

Thus, the radiation pressure due to the shot noise introduces a deviation in the oscillator position $\Delta x_{SN}(\omega)$

$$\Delta x_{SN}(\omega) = |\chi(\omega)|(1+R)\sqrt{\frac{PhB}{\lambda c}}\cos\theta\,, \tag{3.6}$$

where B is the measurement bandwidth.

Besides quantum noise, laser light contains technical intensity noise which in some cases may limit the measurement sensitivity [90]. For example the spectral density of the technical noise of the HeNe laser used in this work is $S_{tech} = 9 \times 10^{-18}$ W^2/Hz at frequencies below 10 MHz. The uncertainty in the oscillator position due to the additional radiation pressure force induced by technical noise of the laser can be estimated with

$$\Delta x_{tech}(\omega) = |\chi(\omega)|(1+R)\frac{\sqrt{S_{tech}B}}{c}\cos\theta\,. \tag{3.7}$$

3.3 Measurement of small displacements

Monitoring the light reflected from a high-finesse Fabry-Pérot interferometer allows the detection of extremely small changes in the cavity length or, equally, displacements in the position of one mirror of the cavity. The fundamental limit in the detection sensitivity of an interferometric displacement measurement arises from the quantum nature of light [16,37,39]. This limit is called the standard quantum limit (SQL). In measuring the position of a mechanical oscillator with an effective mass m_{eff} at a resonance frequency ω_0, the minimum detectable displacement Δx_{SQL} is given by [37]

$$\Delta x_{SQL} = \sqrt{\frac{\hbar}{2m_{eff}\omega_0}}\,. \tag{3.8}$$

The laser beam that is utilized as an interferometric probe beam to detect oscillator displacements contains intrinsic quantum fluctuations in intensity and phase. The quantum noise in the intensity of the probe beam introduces an oscillator displacement through radiation pressure, which is referred to as quantum back action (QBA) of the measurement. At optical resonance, the total optical power P_c circulating inside a low-loss Fabry-Pérot cavity compared to the incident power P_i is given by [91]

$$\frac{P_c}{P_i} = \frac{t_1 t_2}{(1-r_1 r_2)^2} = \frac{1-R}{(1-R)^2} \approx \frac{\mathcal{F}}{\pi}\,, \tag{3.9}$$

where t_1 and t_2 are the amplitude transmission coefficient, r_1 and r_2 are the amplitude reflection coefficient, R is the power reflection coefficient of the two cavity mirrors

($t_1 \approx t_2$ and $r_1 \approx r_2$) and $\mathcal{F}$ is the finesse of the cavity. In other words, the optical power inside the cavity is enhanced by the finesse and an estimate for the uncertainty in the oscillator position due to the quantum back action can be written as

$$\Delta x_{\mathrm{QBA}}(\omega) \approx |\chi(\omega)|(1+R)\sqrt{\frac{P_{\mathrm{i}} hB}{\lambda c}}\frac{\mathcal{F}}{\pi}. \tag{3.10}$$

The quantum phase noise of the probe beam, on the other hand, leads to an uncertainty in the position measurement [16,39]. The quantum phase noise corresponds to the equation

$$\Delta x_{\mathrm{PN}} \approx \sqrt{\frac{hc\lambda B}{P_{\mathrm{i}}}}\frac{1}{4\mathcal{F}}. \tag{3.11}$$

Figure 3.1 illustrates the oscillator displacement noise due to the quantum nature of light as a function of incident laser power. Here, the actual experimental parameters of the PDH-stabilized optomechanical sensor were used (see chapter 4.2). It is worth noting that the displacement noise due to the quantum back action is proportional to the square root of the laser power $P^{½}$, whereas the quantum phase noise leads to a measurement uncertainty which is inversely proportional to the square root of the laser power, $P^{-½}$. The total uncertainty Δx_{tot} in the displacement measurement is a quadrature sum $\Delta x_{\mathrm{tot}}^2 = \Delta x_{\mathrm{QBA}}^2 + \Delta x_{\mathrm{PN}}^2$. The best measurement accuracy is obtained with the optical power that minimizes the sum of the noise terms due to the quantum back action and the quantum phase noise. This optimum power level gives a minimum uncertainty in the oscillator position measurement which is of the order of the SQL. However, at room temperature experiments the quantum noise is typically buried under thermal noise (Δx_{th} in figure 3.1). Oscillator displacement due to the thermal excitation can be derived from equation 2.8,

$$\Delta x_{\mathrm{th}}(\omega) = |\chi(\omega)|\sqrt{\frac{4k_{\mathrm{B}}Tm_{\mathrm{eff}}\omega_0 B}{Q}}. \tag{3.12}$$

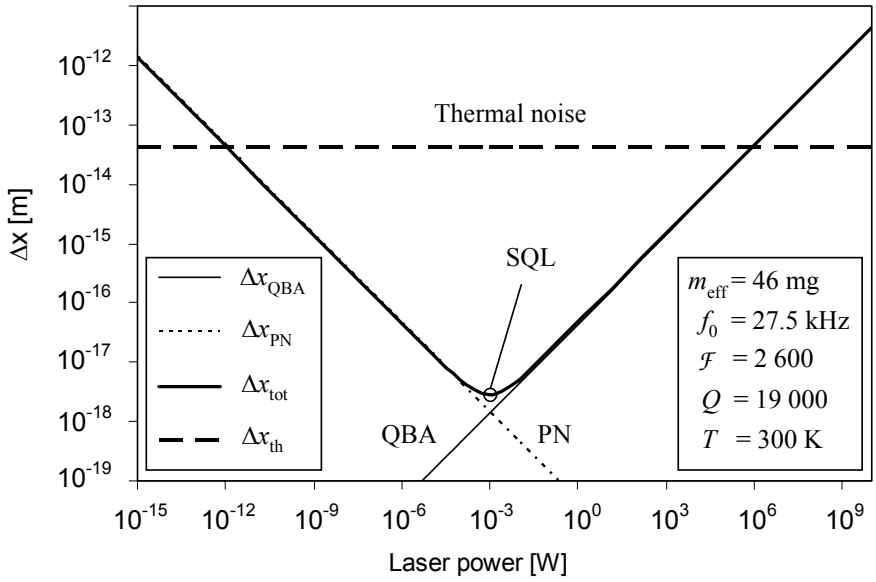

Figure 3.1 Oscillator displacement noise due to the quantum back action (QBA), quantum phase noise (PN) and thermal excitation (th) at room temperature. Experimental parameters of the PDH-stabilized optomechanical sensor were used (see Chapter 4.2). In this case, the optimum laser power level minimizing the quantum-based noise and corresponding to the SQL is of the order of a milliwatt.

3.4 Optical actuation

Optical actuation of mechanical components is typically provided by intensity-modulated and focused laser light. Thus, the exciting force is directly applied to the chosen part of the component without the need of using any additional transducers. The optical actuation is non-contact in nature but, on the other hand, requires direct beam access. Optical actuation is performed either through radiation pressure or by photothermal effects. Radiation pressure has been used for example in optical levitation of small particles [92] and in laser cooling and trapping of atoms and molecules [93,94]. Radiation pressure, *i.e.* the transfer of the momentum of light, inherently introduces very weak forces that are typically not sufficient to produce observable displacements of macroscopic objects. Therefore, optical actuation is typically applied to very small devices such as micromechanical cantilevers [24,25,95-101]. It has been proposed that an array of optically actuated micromechanical devices could be used in such applications as large-bandwidth photodetectors, miniaturized spectrum analyzers, polarization analyzers and even in optical computing [102]. Optical actuation can also be utilized in performing on-wafer testing, analyzing and dynamic measurements of micromechanical components during the fabrication process.

Both radiation pressure and photothermal effect induced actuations of macroscopic mechanical oscillators were studied and demonstrated within this Thesis [II]. Optical actuation measurements were carried out at low pressure ($p \sim 0.1$ mbar) because the

weak effects related to optical actuation would be buried under gas damping at atmospheric pressure. In demonstrating the optical actuation through radiation pressure, the intensity-modulated laser beam was focused onto the HR-coated surface of the torsional silicon oscillator so that most of the incident light was reflected and the number of absorbed photons was small. In order to excite the torsional mode of oscillation, the laser beam was focused 1 mm aside from the torsional axis of the oscillating vane. Figure 3.2 shows the frequency response of the torsional oscillation to the radiation pressure induced by a 1.5 mW intensity-modulated laser beam when the modulation frequency was swept over the mechanical resonance. At resonance, the oscillation amplitude was $\Delta x_{\mathrm{rad}} = 1.4$ pm. In comparison, the resonance was mechanically excited by using a piezo actuator and the magnitude of the piezo actuation was normalized to give a similar oscillation amplitude as the radiation pressure.

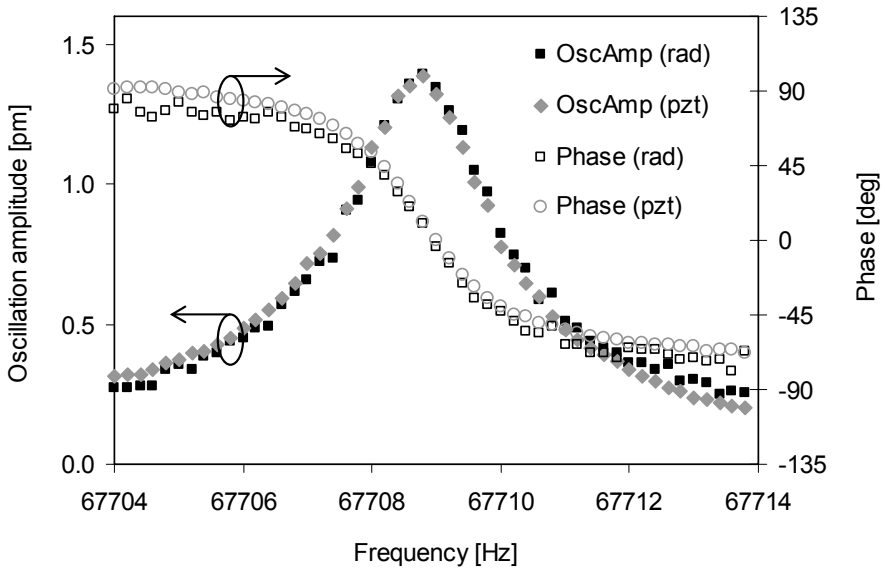

Figure 3.2 Optical actuation through radiation pressure results in a similar frequency response if compared to a normalized mechanical piezo actuation.

The photothermal effect introduces thermoelastic expansion of the solid lattice that arise from heating of the oscillator due to the absorbed photons [103-105]. Typically, a focused laser beam heats the localized spot and the temperature gradient leads to a deformation and bending of the oscillator via thermal expansion. The magnitude of the photothermal effect depends strongly on the ambient temperature, material parameters, geometric dimensions of the oscillator structure and spot size and position of the actuating laser beam [25,95-96].

In order to study optical actuation through the photothermal effect, the intensity modulated laser beam was focused on the uncoated back side of the torsional silicon oscillator. In this configuration, about two-thirds of the incident optical power was

absorbed by the silicon surface ($R_{Si} = 0.35$ at $\lambda = 633$ nm). Again, the laser beam was focused 1 mm aside from the torsional axis in order to provide an exciting torque for the torsional oscillation. Radiation pressure is still involved but it is now substantially weaker than with the HR-coated surface. Figure 3.3 shows the frequency response of the torsional oscillator when the modulation frequency of a 1.5 mW laser beam was swept over the mechanical resonance. Photothermal effect resulted in an oscillation amplitude of $\Delta x_{ph} = 4.3$ pm at resonance. This result was compared to the frequency response attained by mechanically exciting the torsional oscillation with a piezo actuator. The resonance frequency is slightly decreased because the elastic properties of silicon changes as the absorbed photons heat the oscillator [7].

Silicon absorbs light in the visible part of the optical spectrum and is transparent in the infrared above 1.1 μm [106]. At the HeNe laser wavelength of 633 nm, the frequency dependence on the absorbed dc optical power was measured to be -5.5 ppm/mW. In our case, the absorbed dc optical power increases the effective operating temperature of the torsional silicon oscillator by 0.22 K/mW. Thus, the photothermal heating effect may limit the use of HeNe laser beam as a measuring probe especially in those experiments that require the mechanical silicon oscillators to be operated at very low, subkelvin temperatures. On the other hand, the photothermal effect allows adjusting the resonance frequency of a silicon oscillator to a certain value by changing the effective operating temperature with the incident laser power.

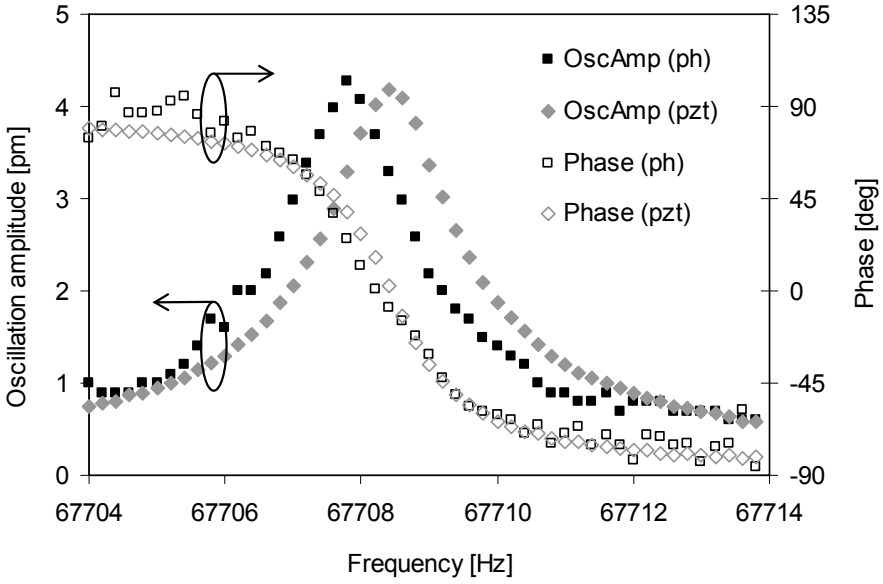

Figure 3.3 The frequency response of the torsional oscillator actuated by a photothermal effect or with a piezo. The resonance frequency is lower in photothermal actuation because the absorbed optical power heats the oscillator leading to the change in the elastic properties of silicon.

In optical actuation experiments, the measured oscillation amplitude depends on various mechanical, thermal and optical effects that are related to the intensity-modulated laser beam, interferometric probe beam and Brownian motion of the silicon oscillator. Oscillator displacements that were measured with the HC-stabilized optomechanical sensor or discussed on a theoretical basis in Publication [II] are listed in table 3.1 and illustrated in figure 3.4. The dashed line in figure 3.4 indicates the sensitivity of the displacement measurement of the HC-stabilized sensor at room temperature, $\Delta x_{\mathrm{min,HC}} = 1.7 \times 10^{-14}$ m.

Table 3.1 Summary of various contributions in the interferometric position measurement of the optical actuation experiment.

Oscillation amplitude [m]	
$\Delta x_{\mathrm{ph}}(\omega_0)$	4.3×10^{-12}
$\Delta x_{\mathrm{rad}}(\omega_0)$	1.4×10^{-12}
$\Delta x_{\mathrm{th}}(\omega_0)$	1.6×10^{-13}
$\Delta x_{\mathrm{rad,dc}}(\omega=0)$	3.6×10^{-17}
Δx_{PN}	3.4×10^{-17}
Δx_{SQL}	1.5×10^{-17}
$\Delta x_{\mathrm{tech}}(\omega_0)$	7.6×10^{-18}
$\Delta x_{\mathrm{QBA}}(\omega_0)$	1.9×10^{-18}
$\Delta x_{\mathrm{SN}}(\omega_0)$	5.5×10^{-20}

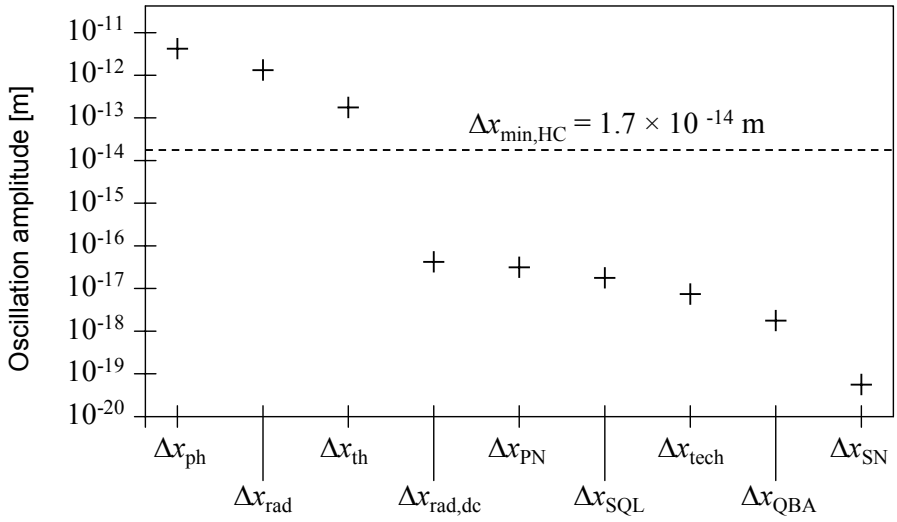

Figure 3.4 The measured oscillation amplitude in optical actuation experiments is a result of various excitation and noise mechanisms. The dashed line indicates the displacement measurement sensitivity of the HC-stabilized optomechanical sensor at room temperature, $\Delta x_{\mathrm{min,HC}} = 1.7 \times 10^{-14}$ m.

4 EXPERIMENTAL SETUPS

Optomechanical sensors allow the detection of ultraweak forces and extremely small displacements in the position of a mechanical oscillator. The motion of the oscillator mirror in a Fabry-Pérot interferometer introduces cavity length variations and, therefore, detuning between the laser frequency and the resonance frequency of the optical cavity. This detuning is typically detected from the light reflected back from the Fabry-Pérot cavity. An active stabilization of the laser frequency improves the stability of the optical resonance and makes it possible to perform extremely sensitive interferometric measurements. The frequency locking of the laser to the optical cavity resonance requires typically the generation of an error signal with a steep slope and a null signal at the optical resonance. The error signal serves as a feedback signal and simultaneously it is used as a measure of dynamic length variations of the optical cavity. Within this Thesis, two different optomechanical sensors were constructed and characterized. The first one is based on the Hänsch-Couillaud (HC) stabilization technique [107] and the other one utilizes the Pound-Drever-Hall (PDH) technique [108].

4.1 Hänsch-Couillaud stabilization

The HR-coated high-Q torsional silicon oscillator was employed as a planar rear mirror in a Fabry-Pérot interferometer which was actively stabilized by using the Hänsch-Couillaud technique [I][II]. In this configuration, a HeNe laser provides linearly polarized 5 mW output power (TEM_{00}) at the wavelength of $\lambda = 633$ nm. The frequency stability of the HeNe laser was earlier measured by comparing it to an additional high-precision iodine stabilized HeNe laser. The electronic feedback circuit of the HC stabilization was observed to be fast enough to compensate the relative cavity length change due to the frequency drift of 100 kHz/s. Laser beam rms intensity noise was less than 0.2 % (<10 MHz) and the polarization ratio was better than 500:1. The power reflectivities of the incoupling mirror and the HR-coated oscillator were $R_1 = 0.99$ and $R_2 = 0.98$, respectively. The optical finesse was $\mathcal{F} = 100$ and it was mainly limited by the losses introduced by the linear polarizer in the cavity. The length of the cavity was 25 mm giving the free spectral range of $\Delta f_{FSR} = 6$ GHz. The width of the optical resonance was $\Delta f_h = 60$ MHz. The radius of curvature of the concave incoupling mirror was 100 mm and the beam waist at the plane oscillator mirror was 93 μm.

Figure 4.1 shows a schematic representation of the Hänsch-Couillaud locking method. This method utilizes polarization spectroscopy in which the changes in the polarization of the reflected light are monitored [107]. Deviation in the phase of the incident laser beam relative to the light field stored inside the optical cavity alters the polarization of the reflected light. The reflected light faces a frequency-dependent elliptical polarization. A polarization analyzer detects dispersion shaped resonances which gives the error signal for the electronic servo loop. The slope of the error signal at optical resonance was determined to be 1.5 nm/V by using the known free spectral range as a length reference. The disadvantage of the Hänsch-Couillaud method is that it requires

an intracavity polarizer which in our configuration was a Brewster plate. Although a Brewster plate possesses low reflection losses, it inevitably limits the obtainable finesse to a rather modest level.

The transmission axis of the intracavity linear polarizer forms an angle θ with the polarization axis of the linearly polarized incident HeNe laser beam (figure 4.1). Thus, the incoming light can be divided into two orthogonal linearly polarized components. One component is parallel and the other one is perpendicular to the transmission axis of the linear polarizer. The parallel component faces a cavity with minimum losses and experiences a frequency-dependent phase shift δ in the reflection. The perpendicular component just reflects from the incoupling mirror and serves as a reference signal. Exactly at resonance ($\delta = 2m\pi$), the reflected intensity has its minimum and the reflected beam is linearly polarized. If the resonance condition is not fulfilled, the reflected parallel component experiences a phase shift relative to the perpendicular component and the reflected beam becomes elliptically polarized. The ellipticity of the polarization is detected with a polarization analyzer which consists of a quarter waveplate and a polarizing beamsplitter.

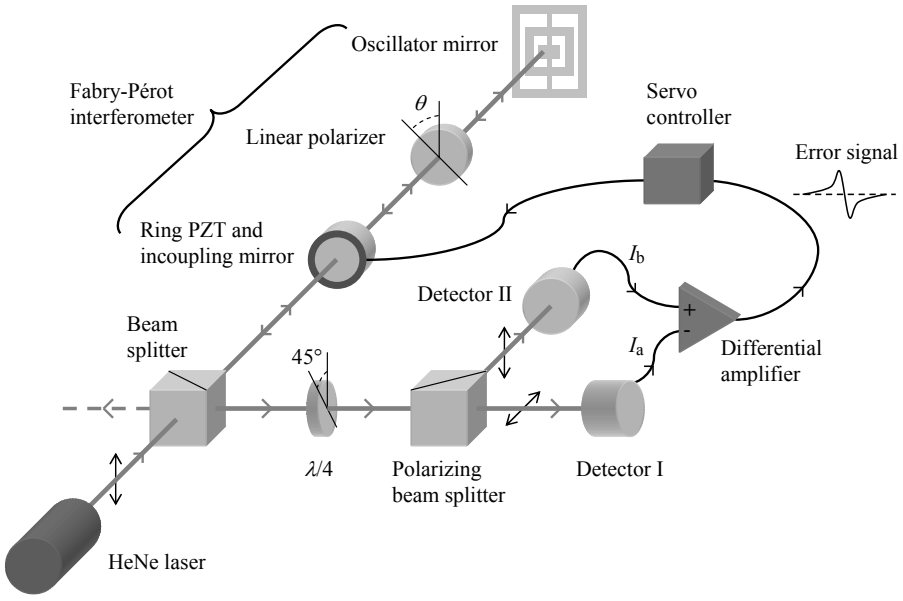

Figure 4.1 The Hänsch-Couillaud locking method was utilized to actively stabilize the Fabry-Pérot interferometer. This technique is based on polarization spectroscopy and the dispersion shaped resonances provide the error signal for the electronic feedback.

The outputs of the polarization analyzer, light intensities I_a and I_b, are detected with silicon photodiodes and connected to a differential amplifier. The output of the differential amplifier provides an error signal with a steep slope at resonance. This error signal is used for the electronic cavity length control and for the analysis of the interferometer response. The mathematical form of the error signal is given by [107]

$$I_a - I_b = I_i 2\cos\theta\sin\theta \frac{T_1 R_{tot}\sin\delta}{(1-R_{tot})^2 + 4R_{tot}\sin^2\left(\frac{\delta}{2}\right)}, \quad (4.1)$$

where I_i is the intensity of the incident laser beam, T_1 is the power transmissivity of the incoupling mirror and R_{tot} is the amplitude ratio between successive roundtrips containing the reflections and any other losses inside the cavity. An ordinary PID controller was used as an electronic feedback servo. It should be noted that the Fabry-Pérot interferometer is sensitive to any length variations of the optical cavity whereas the high-Q oscillator is sensitive only to forces at its mechanical resonance frequency. Therefore, the bandwidth of the electronic feedback must not include the resonance frequency of the mechanical oscillator. Otherwise the cavity stabilization system would try to compensate the cavity length variations due to the high-Q mode oscillation.

It was experimentally demonstrated that a HC-stabilized optomechanical sensor utilizing a HR-coated torsional mode high-Q silicon oscillator as a moving cavity mirror can be used in high-precision sensing applications [I][II]. The sensitivity of the HC-stabilized optomechanical sensor to detect small displacement in the silicon oscillator position is $\Delta x_{min,HC} = 1.7 \times 10^{-14}$ m, which corresponds to the resonant excitation force of the order of 0.1 pN acting on the mechanical oscillator. This high measurement sensitivity is better than the level of thermally excited Brownian motion of the high-Q torsional mode oscillation ($\Delta x_{th} = 1.6 \times 10^{-13}$ m) at room temperature.

4.2 Pound-Drever-Hall stabilization

In the second optomechanical sensor configuration, the moving cavity mirror was a HR-coated high-Q mechanical silicon oscillator vibrating in a non-tilting out-of-plane mode. The benefit of this novel oscillator, if compared to traditional torsional, flexural and many bulk acoustic mode oscillators, is that the action of weak forces is observed to cause only pure linear translation of the moving mirror without any tilting or deformation of the mirror surface. The length of the optical cavity was 13 mm giving a free spectral range of $\Delta f_{FSR} = 11.5$ GHz. The experimentally determined width of the optical resonance was $\Delta f_h = 4.4$ MHz and the optical finesse was $\mathcal{F} = 2\,600$. The spherical concave incoupling mirror had a radius of curvature of 0.5 m and reflectivity of $R_1 = 0.9999$. The reflectivity of the HR-coated oscillator mirror was determined to be $R_2 = 0.9977$. The beam waist at the oscillator mirror was 164 μm. A cw single frequency (TEM_{00}) linearly polarized diode-pumped Nd:YAG laser ($\lambda = 1064$ nm) was used as a light source. Nd:YAG laser was chosen instead of HeNe laser because silicon is transparent in the infrared region and, therefore, the unwanted heating of the oscillator mirror due to the photothermal effect can be avoided. The laser was intensity stabilized and the resulting rms intensity noise was less than 0.1 % (<10 MHz). The laser linewidth was less than 5 kHz (over 1 ms) and the frequency drift was less than 50 MHz/hour at a constant temperature. The optical power entering the high-finesse cavity was 2 mW. In order to decouple the high-Q mode oscillation from gas damping

and acoustic noise, the optical cavity was housed inside a vacuum chamber and the measurements were performed at low pressure ($p \sim 0.1$ mbar).

The Nd:YAG laser frequency was actively stabilized to the resonance of the optical cavity by using the Pound-Drever-Hall (PDH) technique (figure 4.2) [108-110]. The benefit of this technique, if compared to the Hänsch-Couillaud stabilization method, is that it does not require any additional intracavity components that inevitably introduce optical losses. Thus, typically much higher values of optical finesse can be achieved. In PDH technique, the incident light is phase-modulated by an electro-optic modulator (EOM) to produce sidebands at an offset frequency of $f_m = \omega_m / 2\pi = 9.225$ MHz. A polarizing beam splitter and a quarter-wave plate are used as an optical circulator and the light reflected from the high-finesse cavity is detected with a photodiode. The photodiode output is demodulated and low-pass filtered. This results in an error signal which is proportional to the detuning of the laser frequency from the cavity frequency. Thus the error signal contains information about the length variations of the optical cavity. The vibration of the oscillator mirror at the high-Q mode resonance frequency is traced by monitoring the error signal with the phase sensitive (lock-in) detection. The low-frequency part of the error signal serves as a feedback signal to stabilize the laser frequency to the average cavity frequency. The sensitivity of the mirror displacement measurement using the PDH-stabilized optomechanical sensor is $\Delta x_{\mathrm{min,PDH}} = 5 \times 10^{-15}$ m with a 1 Hz bandwidth. If compared to that of the HC-stabilized optomechanical sensor, the measurement sensitivity was increased by one order of magnitude mainly due to the increase in the optical cavity finesse.

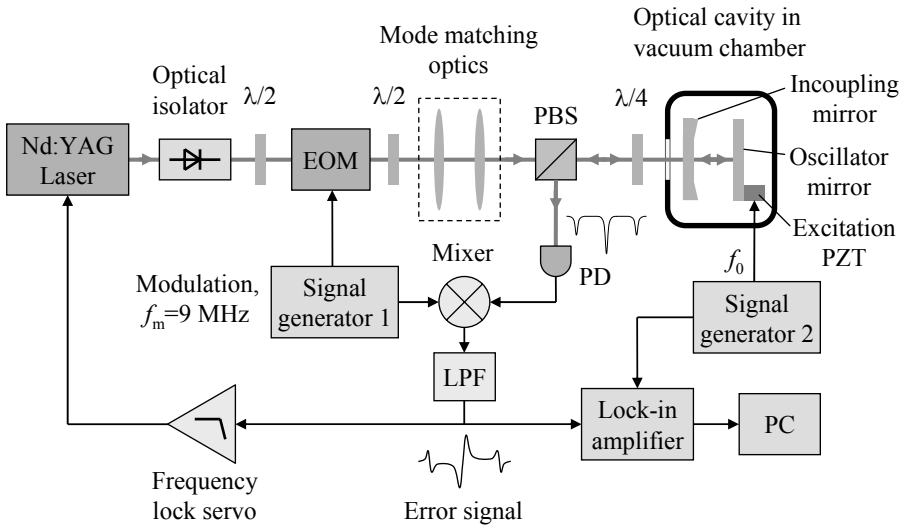

Figure 4.2 The optomechanical sensor configuration and Pound-Drever-Hall stabilization scheme. The high-finesse cavity is housed inside a vacuum chamber in order to decouple the mechanical high-Q mode from external mechanical noise sources. The symbol EOM stands for the electro-optic modulator, PBS for the polarizing beam splitter, PD for the photodiode and LPF for the low-pass filter.

When the electric field of a monochromatic laser beam, $E_i = E_0 e^{i\omega t}$, is incident on a lossless optical cavity, it faces a frequency-dependent reflection according to

$$E_r = r(\omega)E_i = \frac{\sqrt{R_2}\,e^{i(\omega/\Delta f_{FSR})} - \sqrt{R_1}}{1 - \sqrt{R_1 R_2}\,e^{i(\omega/\Delta f_{FSR})}} E_i , \tag{4.2}$$

where $r(\omega)$ is the complex amplitude reflection coefficient of the cavity, R_1 and R_2 are the power reflectivities of the incoupling mirror and oscillator mirror, respectively, and the free spectral range is determined by the cavity length, $\Delta f_{FSR} = c / 2L$. The intensity of the reflected light is given by $|E_r(\omega)|^2$ which corresponds to the inverse of the Airy function. If the incident light is phase-modulated at frequency ω_m and with a modulation depth β, the electric field of the light becomes

$$E_i = E_0 e^{i[\omega t + \beta \sin(\omega_m t)]} . \tag{4.3}$$

If the modulation depth is small ($\beta < 1$), the modulated light field entering the optical cavity contains only a strong carrier component at frequency ω and weak first-order sidebands at frequencies $\omega \pm \omega_m$. Almost all of the optical power lies in the carrier signal and in the first-order sidebands. Therefore, the higher-order sidebands can be neglected to a very good approximation. Using the series expansion by Bessel functions $J_n(\beta)$, equation (4.3) can be written as

$$E_i \approx E_0 \left[J_0(\beta) e^{i\omega t} + J_1(\beta) e^{i(\omega+\omega_m)t} - J_1(\beta) e^{i(\omega-\omega_m)t} \right]. \tag{4.4}$$

The modulated light consists of three frequency components each of which has a reflection coefficient at the appropriate frequency. Thus, the total reflected beam is

$$E_r = E_0 \left[r(\omega) J_0(\beta) e^{i\omega t} + r(\omega+\omega_m) J_1(\beta) e^{i(\omega+\omega_m)t} - r(\omega-\omega_m) J_1(\beta) e^{i(\omega-\omega_m)t} \right]. \tag{4.5}$$

The output of the photodiode is proportional to the intensity of the reflected light, $I_r = |E_r|^2$, which can be written as

$$\begin{aligned} I_r = {} & I_c |r(\omega)|^2 + I_s |r(\omega+\omega_m)|^2 + I_s |r(\omega-\omega_m)|^2 \\ & + 2\sqrt{I_c I_s} \left\{ \mathrm{Re}\left[r(\omega) r^*(\omega+\omega_m) - r^*(\omega) r(\omega-\omega_m) \right] \cos(\omega_m t) \right\} , \\ & + 2\sqrt{I_c I_s} \left\{ \mathrm{Im}\left[r(\omega) r^*(\omega+\omega_m) - r^*(\omega) r(\omega-\omega_m) \right] \sin(\omega_m t) \right\} \\ & + (2\omega_m \text{ terms}) \end{aligned} \tag{4.6}$$

where $I_c = J_0^2(\beta) I_0$ is the light intensity in the carrier and $I_s = J_1^2(\beta) I_0$ is the intensity in each first-order sideband. The upper curve in figure 4.3 illustrates a resulting reflected intensity $I_r(\omega)$ when the modulation depth is $\beta = 0.5$, modulation frequency is $f_m = \omega_m / 2\pi = \Delta f_{FSR} / 20$ and the cavity finesse is $\mathcal{F} = 300$. The lower curve in figure 4.3 represents the corresponding error signal, $S_{Err}(\omega)$. The error signal is obtained by mixing

the photodiode output corresponding to equation (4.6) with the modulation signal at ω_m and finally low-pass filtering the demodulated signal. The resulting error signal can be estimated according to [111]

$$S_{Err} = 2\sqrt{I_c I_s}\,\mathrm{Im}\left[r(\omega)r^*(\omega+\omega_m) - r^*(\omega)r(\omega-\omega_m)\right]. \tag{4.7}$$

When the detuning of the laser frequency from the cavity resonance δf is much smaller than the linewidth of the cavity (*i.e.* $\delta f << \Delta f_h$), the error signal is linear and directly proportional to the detuning. Near resonance, the error signal becomes

$$S_{Err} = -8\sqrt{I_c I_s}\,\frac{2L}{c}\mathcal{F}\delta f\,. \tag{4.8}$$

The slope of the error signal at resonance is an important measure of the detection sensitivity of the fluctuations in the laser frequency or, equivalently, in the cavity length. Equation (4.8) reveals that high-precision measurements favor the use of high-finesse cavities. A more detailed analysis of the PDH technique can be found for example in Ref. [111].

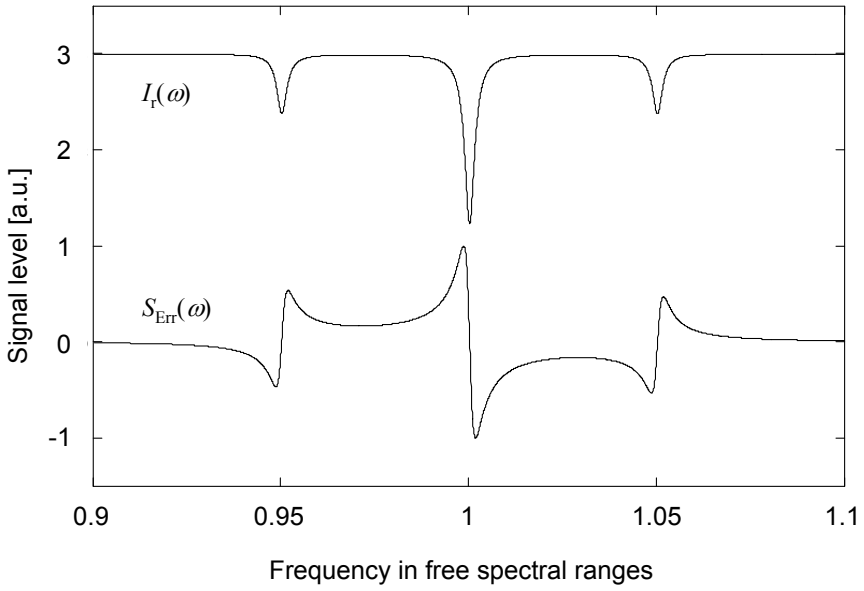

Figure 4.3 The upper curve illustrates the intensity of the phase-modulated light reflected by an optical cavity when the modulation depth is 0.5, modulation frequency is 5 % of the free spectral range and cavity finesse is 300. The lower curve represents the corresponding error signal. The intensity curve and the error signal shown here were calculated using equations (4.6) and (4.7), respectively.

4.3 Michelson interferometry

The construction and implementation of an optomechanical sensor is rather laborious requiring the installation and adjusting of a large set of mechanical, electrical and optical components and devices. In addition, a mechanical silicon oscillator, which is used as a moving cavity mirror, typically needs to be HR-coated on the front surface to provide sufficient reflection. Therefore, in many cases, it is more practical to use other methods to test and characterize the microfabricated mechanical oscillators. In this work, also Michelson interferometry was used to perform additional dynamic analysis and mode pattern measurements of the silicon oscillators.

In the Michelson interferometer configuration used in this work (figure 4.4) an uncoated mechanical silicon oscillator was acting as a moving mirror in one of the interferometer arms. The output intensity of the Michelson interferometer I_{tot} depends on the position of the moving mirror relative to the stationary reference mirror as the phase difference between the two reflected light fields is changed. In this case, the stationary reference mirror is also a piece of polished silicon so that the two reflected interfering light fields have similar intensities, $I_1 = I_2$, giving the maximum modulation depth at the output. The output intensity is

$$I_{\mathrm{tot}}(\Delta x) = \frac{R}{2}\left[I_0 + I_0 \cos\left(\frac{4\pi\Delta x}{\lambda} \right) \right], \tag{4.9}$$

where R is the power reflectivity of the polished silicon surface and I_0 is the intensity of the incident light. The beamsplitter is considered lossless. The silicon oscillator was mechanically excited by using a piezo actuator which was attached to the oscillator mount. In order to guarantee that the interferometer response takes place in the linear region (figure 4.4), the equilibrium position of the oscillator should correspond to the average output intensity I_{ave}, and the oscillation amplitude Δx should be small compared to the wavelength of light ($\Delta x << \lambda$). Therefore, an additional piezo-driven translation stage was utilized to control the oscillator equilibrium position in the x-direction and the magnitude of the oscillator excitation was kept at a moderate level. The oscillator displacements were measured by monitoring the photodiode output with the phase sensitive detection. If compared to HC- and PDH-stabilized optomechanical sensors, the displacement measurement sensitivity of the Michelson interferometer is substantially lower but it still easily allows the detection of picometer-level displacements in the position of the mechanical silicon oscillator.

The oscillator was also attached to a two-dimensional translation stage. Surface scanning by altering the position of the laser probe beam in the yz-plane makes it possible to measure the position-dependent oscillator displacements and thus generating a vibrational mode pattern of the oscillation. Figure 4.5 shows a typical result of a mode pattern measurement of a non-tilting out-of-plane mode oscillator. Each small square in figure 4.5 corresponds to one measurement point and, in this case, 100 μm steps in the y- and z-directions were used.

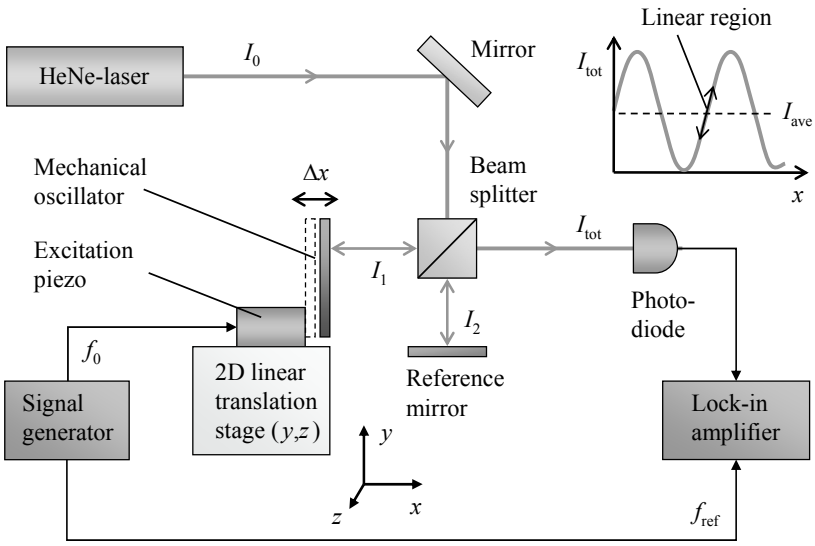

Figure 4.4 Michelson interferometer was used to perform accurate displacement and vibrational mode pattern measurements of microfabricated mechanical silicon oscillators.

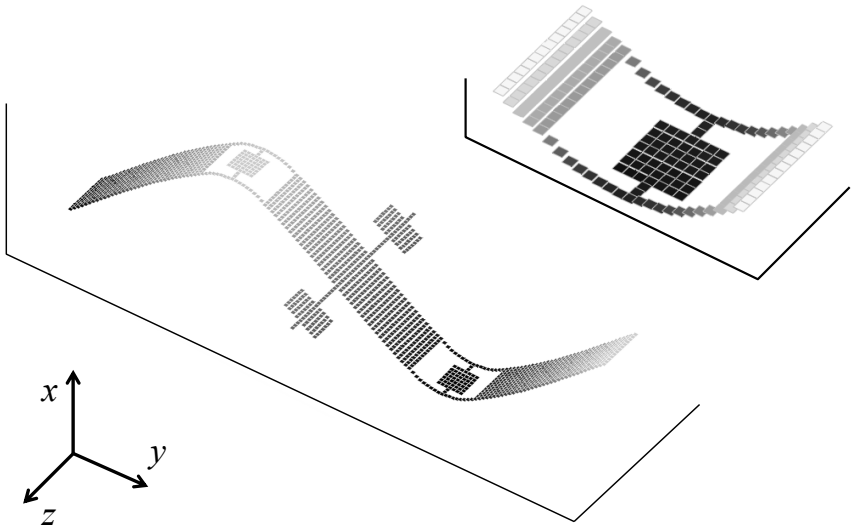

Figure 4.5 The actual mode pattern of a non-tilting out-of-plane mode oscillator was measured by scanning an interferometric probe beam over the oscillator area in the y- and z-directions and reading the position-dependent oscillation amplitudes. The inset shows an enlarged picture of one of the oscillator vanes. The measured mode pattern is in a very good agreement with the FEM simulation result shown in figure 2.6(b).

5 DISCUSSION

During the last three decades, there has been a lot of research activity in the field of measurement of weak forces coupled to a harmonic oscillator and resulting small mechanical displacements [5,37,112]. The reason for the interest in this emerging field arises from both fundamental and technological aspects. First of all, the recent progress in technology has allowed the development and construction of extremely sensitive displacement sensors whose sensitivity is reaching the regime where performing measurements at the quantum level and experimentally demonstrating true quantum effects should be feasible. Such effects are for example the quantum ground state of a mechanical oscillator [36,113], the standard quantum limit (SQL) of a displacement measurement [16] and the quantum back action (QBA) of a laser probe beam [37]. Also the development of gravitational wave detectors (LIGO [86], VIRGO [114], GEO 600 [115], TAMA 300 [116] etc.) has been a significant motivator for the research efforts in this field. Secondly, micro- and nanotechnologies are more often utilized in new applications for high-precision sensing and scientific instrumentation. The dimensions of the structures, trenches, gaps and other features of such devices are typically extremely small meaning that numerous physical phenomena may have an influence that is quite different from the macroworld case [117]. At the micro- and nanoscale, for example the short-range interaction of the surfaces, gas damping, electrostatic forces, radiation pressure of the incident light, friction and sticking become more crucial whereas the importance of gravitational mass disappears. For example, capacitive measurement scheme may become problematic even in tens of nanometer scale since the spatial distribution of charges, charge diffusion and even the Casimir force may reduce the usability of capacitive coupling without introducing novel passivation layers etc. Therefore the studying, developing and analyzing of new kinds of micro- and nanosystems require very sensitive and accurate measurement procedures that provide information and understanding of the physics of the microworld.

Despite all efforts, reaching the SQL in an interferometric position measurement of a mechanical body has not yet been reported. One potential candidate for a quantum-limited displacement sensing is the measurement technique in which the displacement of a nanometer-scale mechanical oscillator is monitored at cryogenic temperatures using a single-electron transistor (SET) [12,118,119]. The benefit of utilizing very small and stiff resonant structures is the fact that the required regime where $k_B T < \hbar\omega_0$ is naturally easier to reach with high frequency systems. In addition, equation (3.8) shows that the SQL is inversely proportional to the square root of the oscillator mass, which favors the use of small-sized oscillators. On the other hand, even more sensitive displacement sensors can be realized by utilizing optical interferometry [34-36]. However, the use of optical interferometric techniques is typically limited to larger resonant structures. Therefore, one should find an optimal compromise between the oscillator size (*i.e.* small mass and high frequency) and low noise detection technique giving the best displacement measurement sensitivity. Table 5.1 shows an overview of various experiments for ultrasensitive displacement detection of mechanical oscillators. The comparison between different experiments is not always straightforward because the

experimental parameters and detection techniques vary a lot from each other. However, the last column in table 5.1 shows the ratio of the displacement measurement sensitivity and theoretical SQL which gives an estimate for how close the quantum-limited behavior is in a given experiment.

Table 5.1 Summary of the experimental parameters of various high-precision displacement measurements. S_{min} is the spectral density of the detection sensitivity (displacement equivalent noise). The last column gives an estimate for the minimum displacement resolution relative to the SQL. TKK (a) and TKK (b) refer to the HC- and PDH-stabilized optomechanical sensors presented in this Thesis, respectively.

Reference	Method	m_{eff} [kg]	f_0	S_{min} [m/Hz$^{1/2}$]	Q	$\Delta x_{min} / \Delta x_{SQL}$
Univ. Moscow [120]	Capacitive	5×10^{-2}	40 kHz	6×10^{-19}	n.a.	3.3×10^{3}
IBM, Cal (a) [42]	Fibre optic int.	2.2×10^{-11}	33.6 kHz	1×10^{-14}	n.a.	1.0×10^{3}
IBM, Cal (b) [121]	Fiber optic int.	3×10^{-13}	5 kHz	1×10^{-11}	86 000	3.2×10^{1}
TKK (a) [I]	Interferometric	5.9×10^{-7}	67.7 kHz	1×10^{-14}	42 100	1.2×10^{3}
TKK (b) [IV]	Interferometric	4.6×10^{-5}	27.5 kHz	4×10^{-15}	19 000	1.9×10^{3}
Univ. Konstanz [34]	Interferometric	1.0×10^{-5}	26 kHz	2×10^{-16}	300 000	1.0×10^{1}
LKB, Paris (a) [35]	Interferometric	2.3×10^{-4}	1.9 MHz	2×10^{-19}	44 000	1.0×10^{1}
LKB, Paris (b) [36]	Interferometric	1.9×10^{-7}	814 kHz	4×10^{-19}	5 000	1.4×10^{0}
Caltech (a) [122]	Magnetomotive	1×10^{-11}	1 MHz	3×10^{-15}	20 000	2.3×10^{1}
Caltech (b) [123]	Piezoelectric	5.2×10^{-17}	11 MHz	3×10^{-13}	2 600	1.6×10^{2}
Univ. California [12]	SET	2.8×10^{-15}	117 MHz	2×10^{-15}	1 700	1.0×10^{2}

According to equation (3.8), the SQL corresponds to $\Delta x_{SQL} = 3 \times 10^{-18}$ m for our non-tilting out-of-plane mode oscillator. This value is more than one thousand times smaller than the present displacement measurement sensitivity of our PDH-stabilized optomechanical sensor. As discussed above, the quantum-limited regime comes closer if the mass of the oscillator is decreased. By using for example silicon-on-insulator (SOI) technology, our non-tilting out-of-plane mode oscillator design could be miniaturized at least with a scaling factor of 1:50. Consequently, the effective mass of the high-Q oscillation mode could be reduced down to a few hundreds of nanograms. The resonance frequency of the high-Q oscillator is inversely proportional to the body length if the aspect ratio is kept constant. Thus, the resonance frequency of the order of one megahertz could be achieved. The displacements of this small oscillator could be measured with a high sensitivity for example by using homodyne Michelson interferometry [124] or optical fiber-based interferometry [121,125].

The deposition of a multi-stack dielectric coating is required in order to achieve a high-reflectivity mirror on a high-Q silicon oscillator leading to a high finesse of the optical cavity. The surface roughness of a polished silicon wafer can be at best of the order of a few angstroms. This good surface quality allows the deposition of highly reflecting and low loss mirror coatings and, therefore, cavity finesses of several tens of thousands can be achieved [34,36]. Unfortunately, additional coatings typically impair the mechanical quality of the resonance [2,83,126]. One possibility to retain the high mechanical quality is to deposit a dielectric mirror whose area is only slightly larger than the spot

size of the interferometric laser probe beam leaving most of the oscillator area and especially the sensitive supporting areas uncoated. However, such mirror patterning requires using of a specific mask during the mirror deposition and such procedure can be very challenging to implement for small micromechanical components. On the other hand, the studies presented in Publication [V] have shown that atomic layer deposition (ALD) technique can be used to deposit high-quality optical thin films that potentially introduce only very low mechanical losses on microfabricated resonant structures. In conclusion, the three key improvements to increase the displacement measurement sensitivity of our optomechanical sensors close to the quantum-limited region are the miniaturization of the mechanical oscillator, performing the measurements at subkelvin temperature and development of the HR-coating that does not degrade the initially high mechanical quality of the oscillator.

6 SUMMARY

In this Thesis, the potential of using optomechanically coupled high-Q mechanical silicon oscillators in high-precision sensing experiments has been studied. Two very sensitive optomechanical sensors, that are operated at low pressure and at room temperature, have been designed, constructed and characterized. The first sensor setup utilizes a microfabricated, high-reflectivity coated torsional high-Q mechanical silicon oscillator as a moving rear mirror in a Fabry-Pérot interferometer. In this configuration, the position of the oscillator mirror is measured by using the Hänsch-Couillaud stabilization technique. In the second sensor setup, a novel non-tilting out-of-plane mode high-Q mechanical silicon oscillator is employed as a moving cavity mirror. This time, the measurement of the mirror position is realized by using the Pound-Drever-Hall technique which actively stabilizes the laser frequency to the optical cavity. The measurement sensitivity was increased by one order of magnitude from the first sensor configuration mainly due to the increase in the optical cavity finesse. The PDH-stabilized sensor setup allows the detection of femtometer-level displacements in the position of the mechanical silicon oscillator. In addition, prospects of using optomechanically coupled macroscopic oscillators for observing even smaller displacements or reaching the standard quantum limit in an interferometric position measurement have been discussed.

The first sensor setup was used to experimentally demonstrate that the mechanical resonance of a macroscopic high-Q oscillator can be optically actuated by using an intensity-modulated laser beam with a very moderate optical power of 1.5 mW. Optical actuation takes place through radiation pressure and photothermal effects, both of which were demonstrated. Optical actuation allows remote excitation and direct utilization of optical power without the need of using any additional transducers such as electrodes for capacitive coupling or piezo actuators for mechanical actuation. The experiments presented in this Thesis demonstrate that optical actuation combined with sensitive optical interferometric measurements can be utilized for example to perform versatile dynamic vibration analysis and testing of micromechanical components. The absorbed HeNe laser light at the wavelength of $\lambda = 633$ nm was observed to heat the silicon oscillator leading to a change in the elastic properties of silicon and decrease in the resonance frequency. The frequency dependence on the absorbed optical power was measured to be -5.5 ppm/mW. This photothermal heating effect may limit the use of HeNe (and other visible region) laser beam as a measuring probe especially in experiments that require the mechanical oscillators to be operated at very low, even subkelvin temperatures. On the other hand, the mechanical resonance frequency can be controlled or locked to a certain value very accurately by adjusting the effective operating temperature with the dc level of the incident laser power.

For the PDH-stabilized sensor setup, a novel high-Q mechanical oscillator, which effectively vibrates in a non-tilting out-of-plane mode, was designed, fabricated and characterized. The benefit of this design, if compared to traditional flexural, torsional and many bulk acoustic mode oscillators, is that the cavity length variations occur due

to the pure linear translation of the cavity mirror without any tilting or deformation of the mirror. The resonance frequency and the Q value of the uncoated oscillators were $f_0 = 27.5$ kHz and $Q = 100\,000$ at low pressure ($p = 10^{-2}$ mbar) and at room temperature. This is the highest reported Q value for a non-tilting out-of-plane mode oscillator. In addition to be used as a moving cavity mirror, this kind of oscillators can be utilized in experiments that require accurate parallel approaching of the well-defined surface even in the near-field regime. The non-tilting behavior is advantageous for example when studying short-range interactions of surfaces, such as Casimir force of two parallel conducting plates. The linear dynamic range of the non-tilting out-of-plane mode oscillation was shown to be very broad corresponding to the oscillation amplitudes at least from $\sim 10^{-14}$ m to $\sim 10^{-6}$ m.

It was demonstrated that atomic layer deposited (ALD) amorphous alumina (Al_2O_3) films with thicknesses at least up to 100 nm can be deposited on microfabricated mechanical resonant structures without any degrading of the initially high mechanical quality of the resonance. This is of great importance when depositing functional, protective and optical thin films on sensitive MEMS devices. This result is very encouraging and should lead to novel ALD applications in MEMS and photonics. Typically, the characteristics of standard lithography and etching processes (such as mask misalignment and over-etching) may cause tiny variations in the dimensions of the microfabricated devices leading to a small deviation from the intended resonance frequency. It was shown that alumina films effectively stiffen the resonant structure leading to the increase in the resonance frequency with increasing the film thickness. Thus, thin alumina films can be used for fine-tuning and trimming of the resonance frequency without decreasing the Q value.

In addition, the resonance frequency of the silicon oscillator was shown to be less sensitive to changes in ambient temperature when the oscillator was coated with alumina and the temperature sensitivity decreases as the film thickness increases. Therefore, alumina coated silicon oscillators are promising candidates for realizing temperature insensitive reference oscillators, sensors and filters. Moreover, it was shown that alumina thin films on silicon substrates can be used as a single-layer anti-reflection coating offering a significant reduction in the reflectivity from $R_{Si} = 0.35$ for a clean silicon surface to $R_{AR} = 0.035$ for a silicon surface with a quarter wavelength alumina coating at $\lambda = 633$ nm.

The results presented in this Thesis validate the great potential of optomechanically coupled high-Q mechanical silicon oscillators in high-precision measurements. In addition, the new knowledge of the effects of atomic layer deposited alumina thin films on the dynamic, thermomechanical and optical characteristics of microfabricated resonant silicon structures can be utilized in developing new sensor applications.

REFERENCES

[1] K. Wang, A.-C. Wong and C. T.-C. Nguyen, "VHF free-free beam high-*Q* micromechanical resonators", *J. Microelectromech. Syst.* **9**, 347 (2000).

[2] R. A. Buser and N. F. de Rooij, "Very high *Q*-factor resonators in monocrystalline silicon", *Sensors Actuators* **A21-A23**, 323 (1990).

[3] T. Mattila, J. Kiihamäki, T. Lamminmäki, O. Jaakkola, P. Rantakari, A. Oja, H. Seppä, H. Kattelus and I. Tittonen, "A 2 MHz micromechanical bulk acoustic mode oscillator", *Sensors Actuators* A **101**, 1 (2002).

[4] R. N. Kleinman, G. K. Kaminsky, J. D. Reppy, R. Pindak and D. J. Bishop, "Single-crystal silicon high-*Q* torsional oscillators", *Rev. Sci. Instrum.* **56**, 2088 (1985).

[5] M. F. Bocko and R. Onofrio, "On the measurement of a weak classical force coupled to a harmonic oscillator: experimental progress", *Rev. Mod. Phys.* **68**, 755 (1996).

[6] J. L. Arlett, J. R. Maloney, B. Gudlewski, M. Muluneh and M. L. Roukes, "Self-sensing micro- and nanocantilevers with attonewton-scale force resolution", *Nano Lett.* **6**, 1000 (2006).

[7] U. Gysin, S. Rast, P. Ruff, E. Meyer, D. W. Lee, P. Vettiger and C. Gerber, "Temperature dependence of the force sensitivity of silicon cantilevers", *Phys. Rev.* B **69**, 045403 (2004).

[8] R. Lifshitz and M. L. Roukes, "Thermoelastic damping in micro- and nanomechanical systems", *Phys. Rev.* B **61**, 5600 (2000).

[9] R. E. Mihailovich and N. C. MacDonald, "Dissipation measurements of vacuum-operated single-crystal silicon microresonators", *Sensors Actuators* A **50**, 199 (1995).

[10] G. Stemme, "Resonant silicon sensors", *J. Micromech. Microeng.* **1**, 113 (1991).

[11] X. Liu, S. F. Morse, J. F. Vignola, D. M. Photiadis, A. Sarkissian, M. H. Marcus and B. H. Houston, "On the modes and loss mechanisms of a high *Q* mechanical oscillator", *App. Phys. Lett.* **78**, 1346 (2001).

[12] R. G. Knobel and A. N. Cleland, "Nanometer-scale displacement sensing using a single electron transistor", *Nature* **424**, 291 (2003).

[13] R. F. Service, "Tipping the scales – just barely", *Science* **312**, 683 (2006).

[14] K. L. Ekinci, Y. T. Yang and M. L. Roukes, "Ultimate limits to inertial mass sensing based upon nanoelectromechanical systems", *J. Appl. Phys.* **95**, 2682 (2004).

[15] T. D. Stowe, K. Yasumura, T. W. Kenny, D. Botkin, K. Wago and D. Rugar, "Attonewton force detection using ultrathin silicon cantilevers", *Appl. Phys. Lett.* **71**, 288 (1997).

[16] C. M. Caves, "Quantum-mechanical radiation-pressure fluctuations in an interferometer", *Phys. Rev. Lett.* **45**, 75 (1980).

[17] Yi Pang and J.-P. Richard, "Room-temperature tests of an optical transducer for resonant gravitational wave detectors", *Appl. Opt.* **34**, 4982 (1995).

[18] J. Hough and S. Rowan, "Laser interferometry for the detection of gravitational waves", *J. Opt. A: Pure Appl. Opt.* **7**, S257 (2005).

[19] G. J. Milburn, K. Jacobs and D. F. Walls, "Quantum-limited measurements with the atomic force microscope", *Phys. Rev.* A **50**, 5256 (1994).
[20] P. F. Cohadon, A. Heidmann and M. Pinard, "Cooling of a mirror by radiation pressure", *Phys. Rev. Lett.* **83**, 3174 (1999).
[21] D. Vitali, S. Mancini, L. Ribichini and P. Tombesi, "Macroscopic mechanical oscillators at the quantum limit through optomechanical cooling", *J. Opt. Soc. Am.* B **20**, 1054 (2003).
[22] A. Schliesser, P. Del'Haye, N. Nooshi, K. J. Vahala and T. J. Kippenberg, "Radiation pressure cooling of a micromechanical oscillator using dynamical backaction", *Phys. Rev. Lett.* **97**, 243905 (2006).
[23] M. Pinard, P. F. Cohadon, T. Briant and A. Heidmann, "Full mechanical characterization of a cold damped mirror", *Phys. Rev.* A **63**, 013808 (2000).
[24] D. R. Koehler, "Optical actuation of micromechanical components", *J. Opt. Soc. Am.* B **14**, 2197 (1997).
[25] O. Marti, A. Ruf, M. Hipp, H. Bielefeldt, J. Colchero and J. Mlynek, "Mechanical and thermal effects of laser irradiation on force microscope cantilevers", *Ultramicroscopy* **42-44**, 345 (1992).
[26] A. Heidmann, Y. Hadjar and M. Pinard, "Quantum nondemolition measurement by optomechanical coupling", *Appl. Phys.* B **64**, 173 (1997).
[27] V. Giovannetti, S. Mancini, P. Tombesi, "Radiation pressure induced Einstein-Podolsky-Rosen paradox", *Europhys. Lett.* **54**, 559 (2001).
[28] S. Manicini, V. Giovannetti, D. Vitali and P. Tombesi, "Entangling macroscopic oscillators exploiting radiation pressure", *Phys. Rev. Lett.* **88**, 120401 (2002).
[29] S. Mancini, D. Vitali, V. Giovannetti and P. Tombesi, "Stationary entanglement between macroscopic mechanical oscillators", *Eur. Phys. J.* D **22**, 417 (2003).
[30] S. Pirandola, S. Mancini, D. Vitali and P. Tombesi, "Continuous variable entanglement by radiation pressure", *J. Opt. B: Quantum Semiclass. Opt.* **5**, S523 (2003).
[31] M. Pinard, Y. Hadjar and A. Heidmann, "Effective mass in quantum effects of radiation pressure", *Eur. Phys. J.* D **7**, 107 (1999).
[32] J.-M. Courty, A. Heidmann and M. Pinard, "Quantum locking of mirrors in interferometers", *Phys. Rev. Lett.* **90**, 083601 (2003).
[33] W. Marshall, C. Simon, R. Penrose and D. Bouwmeester, "Towards quantum superpositions of a mirror", *Phys. Rev. Lett.* **91**, 130401 (2003).
[34] I. Tittonen, G. Breitenbach, T. Kalkbrenner, T. Müller, R. Conradt, S. Schiller, E. Steinsland, N. Blanc and N. F. de Rooij, "Interferometric measurements of the position of a macroscopic body: towards observation of quantum limits", *Phys. Rev.* A **59**, 1038 (1999).
[35] Y. Hadjar, P. F. Cohadon, C. G. Aminoff, M. Pinard and A. Heidmann, "High-sensitivity optical measurement of mechanical Brownian motion", *Europhys. Lett.* **47**, 545 (1999).
[36] O. Arcizet, P. F. Cohadon, T. Briant, M. Pinard, A. Heidmann, J.-M. Mackowski, C. Michel, L. Pinard, O. Francais and L. Rousseau, "High-sensitivity optical monitoring of a micro-mechanical resonator with a quantum-limited optomechanical sensor", *Phys. Rev. Lett.* **97**, 133601 (2006).

[37] V. B. Braginsky and F. Y. Khalili, "Quantum Measurement", (Cambridge University Press, Cambridge, 1992).
[38] K. Jacobs, I. Tittonen, H. M. Wiseman and S. Schiller, "Quantum noise in the position measurement of a cavity mirror undergoing Brownian motion", *Phys. Rev.* A **60**, 538 (1999).
[39] C. Brif and A. Mann, "Quantum statistical properties of the radiation field in a cavity with a movable mirror", *J. Opt. B: Quantum Semiclass. Opt.* **2**, 53 (2000).
[40] A. Heidmann, J.-M. Courty, M. Pinard and J. Lebars, "Beating quantum limits in interferometers with quantum locking of mirrors", *J. Opt. B: Quantum Semiclass. Opt.* **6**, S684 (2004).
[41] R. C. Ritter and G. T. Gillies, "Classical limit of mechanical thermal noise reduction by feedback", *Phys. Rev.* A **31**, 995 (1985).
[42] D. Rugar and P. Grütter, "Mechanical parametric amplification and thermomechanical noise squeezing", *Phys. Rev. Lett.* **67**, 699 (1991).
[43] T. Briant, P. F. Cohadon, M. Pinard and A. Heidmann, "Optical phase-space reconstruction of mirror motion at the attometer level", *Eur. Phys. J.* D **22**, 131 (2003).
[44] P. R. Saulson, "Thermal noise in mechanical experiments", *Phys. Rev.* D **42**, 2437 (1990).
[45] C. L. Spiel, R. O. Pohl and A. T. Zehnder, "Normal modes of a Si(100) double-paddle oscillator", *Rev. Sci. Instrum.* **72**, 1482 (2001).
[46] M. J. Tudor, M. V. Andres, K. W. H. Foulds and J. M. Naden, "Silicon resonator sensors: interrogation techniques and characteristics", *IEE Proc.* **135**, 364 (1988).
[47] K. Y. Yasumura, T. D. Stowe, E. M. Chow, T. Pfafman, T. W. Kenny, B. C. Stipe and D. Rugar, "Quality factors in micron- and submicron-thick cantilevers", *J. Microelectromech. Syst.* **9**, 117 (2000).
[48] B. H. Houston, D. M. Photiadis, M. H. Marcus, J. A. Bucaro, X. Liu and J. F. Vignola, "Thermoelastic loss in microscale oscillators", *Appl. Phys. Lett.* **80**, 1300 (2002).
[49] D. W. Carr, S. Evoy, L. Sekaric, H. G. Craighead and J. M. Parpia, "Measurement of mechanical resonance and losses in nanometer scale silicon wires", *Appl. Phys. Lett.* **75**, 920 (1999).
[50] B. Le Foulgoc, T. Bourouina, O. Le Traon, A. Bosseboeuf, F. Marty, C. Breluzeau, J.-P. Grandchamp and S. Masson, "Highly decoupled single-crystal silicon resonators: an approach for the intrinsic quality factor", *J. Micromech. Microeng.* **16**, S45 (2006).
[51] T. B. Gabrielson, "Mechanical-thermal noise in micromachined acoustic and vibration sensors", *IEEE Trans. Electron Devices* **40**, 903 (1993).
[52] K. E. Petersen, "Silicon as a Mechanical Material", *Proc. IEEE* **70**, 420 (1982).
[53] S. Franssila, "Introduction to Microfabrication", (West Sussex, Wiley, 2004).
[54] S. P. Beeby and M. J. Tudor, "Modelling and optimization of micromachined silicon resonators", *J. Micromech. Microeng.* **5**, 103 (1995).
[55] S. Evoy, D. W. Carr, L. Sekaric, A. Olkhovets, J. M. Parpia and H. G. Craighead, "Nanofabrication and electrostatic operation of single-crystal silicon paddle oscillators", *J. Appl. Phys.* **86**, 6072 (1999).

[56] S. Evoy, A. Olkhovets, L. Sekaric, J. M. Parpia, H. G. Graighead and D. W. Carr, "Temperature-dependent internal friction in silicon nanoelectromechanical systems", *Appl. Phys. Lett.* **77**, 2397 (2000).

[57] H. Haucke, X. Liu, J. F. Vignola, B. H. Houston, M. H. Marcus and J. W. Baldwin, "Effects of annealing and temperature on acoustic dissipation in a micromechanical silicon oscillator", *Appl. Phys Lett.* **86**, 181903 (2005).

[58] L. Haiberger, D. Jäger and S. Schiller, "Fabrication and laser control of double-paddle silicon oscillators", *Rev. Sci. Instrum.* **76**, 04506 (2005).

[59] M. D. Chabot, J. M. Moreland, L. Gao, S.-H. Liou and C. W. Miller, "Novel fabrication of micromechanical oscillators with nanoscale sensitivity at room temperature", *J. Microelectromech. Syst.* **14**, 1118 (2005).

[60] D. W. Carr, S. Evoy, L. Sekaric, H. G. Craighead and J. M. Parpia, "Parametric amplification in a torsional microresonator", *Appl. Phys. Lett.* **77**, 1545 (2000).

[61] S. K. Lamoreaux, "Demonstration of the Casimir force in the 0.6 to 6 μm range", *Phys. Rev. Lett.* **78**, 5 (1997).

[62] V. Petrov, M. Petrov, V. Bryksin, J. Petter and T. Tschudi, "Optical detection of the Casimir force between macroscopic objects", *Opt. Lett.* **31**, 3167 (2006).

[63] U. Mohideen and A. Roy, "Precision measurement of the Casimir force from 0.1 to 0.9 μm", *Phys. Rev. Lett.* **81**, 4549 (1998).

[64] H. B. Chan, V. A. Aksyuk, R. N. Kleiman, D. J. Bishop and F. Capasso, "Quantum mechanical actuation of microelectromechanical systems by the Casimir force", *Science* **291**, 1941 (2001).

[65] H. B. Chan, V. A. Aksyuk, R. N. Kleiman, D. J. Bishop and F. Capasso, "Nonlinear micromechanical Casimir oscillator", *Phys. Rev. Lett.* **87**, 211801 (2001).

[66] L. Meirovitch, "Analytical methods in vibrations", (Macmillan, New York, 1967).

[67] Torsional oscillators were coated at *Optronics Department of Finnish Defence Forces* in Lievestuore (Finland).

[68] Non-tilting out-of-plane mode oscillators were coated at *Oplatek Oy* in Leppävirta (Finland).

[69] C. R. Stoldt and V. M. Bright, "Ultra-thin film encapsulation processes for micro-electro-mechanical devices and systems", *J. Phys. D: Appl. Phys.* **39**, R163 (2006).

[70] N. D. Hoivik, J. W. Elam, R. J. Linderman, V. M. Bright, S. M. George and Y. C. Lee, "Atomic layer deposited protective coatings for micro-electromechanical systems", *Sensors Actuators* A **103**, 100 (2003).

[71] T. M. Mayer, J. W. Elam, S. M. George, P. G. Kotula and R. S. Goeke, "Atomic-layer deposition of wear-resistant coatings for microelectromechanical devices", *Appl. Phys. Lett.* **82**, 2883 (2003).

[72] E. J. Eklund and A. M. Shkel, "Factors affecting the performance of micromachined sensors based on Fabry-Perot interferometry", *J. Micromech. Microeng.* **15**, 1770 (2005).

[73] M. D. Groner, J. W. Elam, F. H. Fabreguette and S. M. George, "Electrical characterization of thin Al_2O_3 films grown by atomic layer deposition on silicon and various metal substrates", *Thin Solid Films* **413**, 186 (2002).

[74] A. C. Dillon, A. W. Ott, J. D. Way and S. M. George, "Surface chemistry of Al_2O_3 deposition using $Al(CH_3)_3$ and H_2O in a binary reaction sequence", *Surf. Sci.* **322**, 230 (1995).
[75] R. L. Puurunen, "Surface chemistry of atomic layer deposition: a case study for the trimethylaluminum/water process", *J. Appl. Phys.* **97**, 121301 (2005).
[76] D. R. G. Mitchell, G. Triani, D. J. Attard, K. S. Finnie, P. J. Evans, C. J. Barbé and J. R. Bartlett, "Atomic layer deposition of TiO_2 and Al_2O_3 thin films and nanolaminates", *Smart Mater. Struct.* **15**, S57 (2006).
[77] A. W. Ott, J. W. Klaus, J. M. Johnson and S. M. George, "Al_2O_3 thin film growth on Si(100) using binary reaction sequence chemistry", *Thin Solid Films* **292**, 135 (1997).
[78] M. K. Tripp, C. Stampfer, D. C. Miller, T. Helbling, C. F. Herrmann, C. Hierold, K. Gall, S. M. George and V. M. Bright, "The mechanical properties of atomic layer deposited alumina for use in micro- and nano-electromechanical systems", *Sensors Actuators* A **130-131**, 419 (2006).
[79] M. Copel, E. Cartier, E. P. Gusev, S. Guha, N. Bojarczuk and M. Poppeller, "Robustness of ultrathin aluminum oxide dielectrics on Si(001)", *Appl. Phys. Lett.* **78**, 2670 (2001).
[80] E. P. Gusev, M. Copel, E. Cartier, I. J. R. Baumvol, C. Krug and M. A. Gribelyuk, "High-resolution depth profiling in ultrathin Al_2O_3 films on Si", *Appl. Phys. Lett.* **76**, 176 (2000).
[81] Z. W. Zhao, B. K. Tay, S. P. Lau and C. Y. Xiao, "Microstructural and optical properties of aluminum oxide thin films prepared by off-plane filtered cathodic vacuum arc system", *J. Vac. Sci. Technol.* A **21**, 906 (2003).
[82] C. R. Stoldt, M. C. Fritz, C. Carraro and R. Maboudian, "Micromechanical properties of silicon-carbide thin films deposited using single-source chemical-vapor deposition", *Appl. Phys. Lett.* **79**, 347 (2001).
[83] R. Sandberg, K. Molhave, A. Boisen and W. Svendsen, "Effect of gold coating on the *Q*-factor of a resonant cantilever", *J. Micromech. Microeng.* **15**, 2249 (2005).
[84] F. Shen, P. Lu, S. J. O'Shea, K. H. Lee and T. Y. Ng, "Thermal effects on coated resonant microcantilevers", *Sensors Actuators* A **95**, 17 (2001).
[85] Y. Zhang, M. L. Dunn, K. Gall, J. W. Elam and S. M. George, "Suppression of inelastic deformation of nanocoated thin film microstructures", *J. Appl. Phys.* **95**, 8216 (2004).
[86] A. Abramovici *et al*., "LIGO: The laser interferometer gravitational-wave observatory", *Science* **256**, 325 (1992).
[87] D. Rugar and P. Hansma, "Atomic force microscopy", *Phys. Today* **43**, 23 (1990).
[88] A. Dorsel, J. D. McCullen, P. Meystre, E. Vignes and H. Walther, "Optical bistability and mirror confinement induced by radiation pressure", *Phys. Rev. Lett.* **51**, 1550 (1983).
[89] P. Mulser, "Radiation pressure on macroscopic bodies", *J. Opt. Soc. Am.* B **2**, 1814 (1985).
[90] O. Svelto, "Principles of Laser", (4th edition, Plenum Press, New York, 1998).
[91] A. E. Siegman, "Lasers", (University Science Books, California, 1986).

[92] A. Ashkin, "Acceleration and trapping of particles by radiation pressure", *Phys. Rev. Lett.* **24**, 156 (1970).
[93] D. J. Wineland and W. M. Itano, "Laser cooling of atoms", *Phys. Rev.* A **20**, 1521 (1979).
[94] C. S. Adams and E. Riis, "Laser cooling and trapping of neutral atoms", *Prog. Quant. Electr.* **21**, 1 (1997).
[95] B. Q. Li, J. Lin, W. Wang, "Thermomechanical deflection of microcantilever beams in scanning force microscopes", *J. Micromech. Microeng.* **6**, 330 (1996).
[96] S. Petitgrand, B. Courbet and A. Bosseboeuf, "Characterization of static and dynamic optical actuation of Al microbeams by microscopic interferometry techniques", *J. Micromech. Microeng.* **13**, S113 (2003).
[97] J. Yang, T. Ono and M. Esashi, "Surface effects and high quality factors in ultrathin single-crystal silicon cantilevers", *Appl. Phys. Lett.* **77**, 3860 (2000).
[98] N. V. Lavrik and P. G. Datskos, "Femtogram mass detection using photothermally actuated nanomechanical resonators", *Appl. Phys. Lett.* **82**, 2697 (2003).
[99] J. Li and S. Evoy, "Study of laser-induced self-oscillations in silicon nanomechanical resonators", *J. Appl. Phys.* **98**, 084316 (2005).
[100] J. E. Graebner, S. Pau and P. L. Gammel, "All-optical excitation and detection of microelectrical-mechanical systems", *Appl. Phys. Lett.* **81**, 3531 (2002).
[101] M. Sulfridge, T. Saif, N. Miller N and K. O'Hara, "Optical actuation of a bistable MEMS", *J. Microelectromech. Syst.* **11**, 574 (2002).
[102] D. Dragoman and M. Dragoman, "Optical actuation of micromechanical tunnelling structures with applications in spectrum analysis and optical computing", *Appl. Opt.* **38**, 6773 (1999).
[103] V. B. Braginsky, M. L. Gorodetsky, S. P. Vyatchanin, "Thermodynamical fluctuations and photo-thermal shot noise in gravitational wave antennae", *Phys. Lett.* A **264**, 1 (1999).
[104] M. Cerdonio, L. Conti, A. Heidmann and M. Pinard, "Thermoelastic effects at low temperatures and quantum limits in displacement measurements", *Phys. Rev.* D **63**, 082003 (2001).
[105] M. De Rosa, L. Conti, M. Cerdonio, M. Pinard and F. Marin, "Experimental measurement of the dynamic photothermal effect in Fabry-Perot cavities for gravitational wave detectors", *Phys. Rev. Lett.* **89**, 237402 (2002).
[106] G. E. Jellison, Jr., F. A. Modine, "Optical absorption of silicon between 1.6 and 4.7 eV at elevated temperatures", *Appl. Phys. Lett.* **41**, 180 (1982).
[107] T. W. Hänsch and B. Couillaud, "Laser frequency stabilization by polarization spectroscopy of a reflecting reference cavity", *Optics Communications* **35**, 441 (1980).
[108] R. W. P. Drewer, J. L. Hall, F. V. Kowalski, J. Hough, G. M. Ford, A. J. Munley and H. Ward, "Laser phase and frequency stabilization using an optical resonator", *Appl. Phys.* B **31**, 97 (1983).
[109] G. C. Bjorklund, "Frequency-modulation spectroscopy: a new method for measuring weak absorptions and dispersions", *Optics Letters* **5**, 15 (1980).
[110] G. C. Bjorklund, M. D. Levenson, W. Lenth and C. Ortiz, "Frequency modulation (FM) spectroscopy", *Appl. Phys.* B **32**, 145 (1983).

[111] E. D. Black, "An introduction to Pound-Drever-Hall laser frequency stabilization", *Am. J. Phys.* **69**, 79 (2001).
[112] M. Blencowe, "Quantum electromechanical systems", *Physics Reports* **395**, 159 (2004).
[113] I. Wilson-Rae, P. Zoller and A. Imamoglu, "Laser cooling of a nanomechanical resonator mode to its quantum ground state", *Phys. Rev. Lett.* **92**, 075507 (2004).
[114] B. Caron *et al*., "The Virgo interferometer", *Class. Quantum Grav.* **14**, 1461 (1997).
[115] B. Willke *et al*., "The GEO 600 gravitational wave detector", *Class. Quantum Grav.* **19**, 1377 (2002).
[116] M. Ando *et al*., "Current status of TAMA", *Class. Quantum Grav.* **19**, 1409 (2002).
[117] C. Hierold, "From micro- to nanosystems: mechanical sensor go nano", *J. Micromech. Microeng.* **14**, S1 (2004)
[118] R. Knobel and A. N. Cleland, "Piezoelectric displacement sensing with a single electron transistor", *Appl. Phys. Lett.* **81**, 2258 (2002).
[119] A. Naik, O. Buu, M. D. LaHaye, A. D. Armour, A. A. Clerk, M. P. Blencowe and K. C. Schwab, "Cooling a nanomechancial resonator with quantum back-action", *Nature* **443**, 193 (2006).
[120] V. B. Braginsky, V. P. Mitrofanov and V. I. Panov, "Systems with small dissipation", (University of Chicago, Chicago, 1985).
[121] H. J. Mamin and D. Rugar, "Sub-attonewton force detection at millikelvin temperatures", *Appl. Phys. Lett.* **79**, 3358 (2001).
[122] P. Mohanty, D. A. Harrington and M. L. Roukes, "Measurement of small forces in micron-sized resonators", *Physica* B **284-288**, 2143 (2000).
[123] H. X. Tang, M. H. Huang, M. L. Roukes, M. Bichler and W. Wegscheider, "Two-dimensional electron-gas actuation and transduction for GaAs nanoelectromechanical systems", *Appl. Phys. Lett.* **81**, 3879 (2002).
[124] J. V. Knuuttila, P. T. Tikka and M. M. Salomaa, "Scanning Michelson interferometer for imaging surface acoustic wave fields", *Opt. Lett.* **25**, 613 (2000).
[125] D. Rugar, H. J. Mamin and P. Guethner, "Improved fiber-optic interferometer for atomic force microscopy", *Appl. Phys. Lett.* **55**, 2588 (1989).
[126] H. R. Böhm, S. Gigan, F. Blaser, A. Zeilinger, M. Aspelmeyer, G. Langer, D. Bäuerle, J. B. Hertzberg and K. C. Schwab, "High reflectivity high-*Q* micromechanical Bragg mirror", *Appl. Phys. Lett.* **89**, 223101 (2006).

ISBN 978-951-22-8978-3
ISBN 978-951-22-8979-0 (PDF)
ISSN 1795-2239
ISSN 1795-4584 (PDF)